Received: 18 July 2020 | Revised: 22 February 2021 | Accepted: 6 April 2021

DOI: 10.1111/bph.15499

RESEARCH PAPER

Acinar cell NLRP3 inflammasome and gasdermin D (GSDMD) activation mediates pyroptosis and systemic inflammation in acute pancreatitis

Lin Gao[1] | Xiaowu Dong[2] | Weijuan Gong[3,4] | Wei Huang[5] | Jing Xue[6] | Qingtian Zhu[3] | Nan Ma[1] | Weiwei Chen[1] | Xianghui Fu[7] | Xiang Gao[8] | Zhaoyu Lin[8] | Yanbing Ding[3] | Juanjuan Shi[6] | Zhihui Tong[1] | Tingting Liu[5] | Rajarshi Mukherjee[9] | Robert Sutton[9] | Guotao Lu[3] | Weiqin Li[1,2]

[1]Center of Severe Acute Pancreatitis (CASP), Department of Critical Care Medicine, Jinling Hospital, Medical School of Nanjing University, Nanjing, China

[2]Center of Severe Acute Pancreatitis (CASP), Department of Critical Care Medicine, Jinling Hospital, Nanjing Medical University, Nanjing, China

[3]Pancreatic Center, Department of Gastroenterology, Affiliated Hospital of Yangzhou University, Yangzhou University, Yangzhou, China

[4]Jiangsu Co-innovation Centre for Prevention and Control of Important Animal Infectious Diseases and Zoonoses, College of Veterinary Medicine, Yangzhou University, Yangzhou, China

[5]Department and Laboratory of Integrated Traditional Chinese and Western Medicine, Sichuan Provincial Pancreatitis Centre and West China-Liverpool Biomedical Research Centre, West China Hospital, Sichuan University, Chengdu, China

[6]State Key Laboratory of Oncogenes and Related Genes, Stem Cell Research Centre, Ren Ji Hospital, School of Medicine, Shanghai Jiao Tong University, Shanghai, China

[7]Division of Endocrinology and Metabolism, State Key Laboratory of Biotherapy, West China Hospital, Sichuan University and Collaborative Innovation Centre of Biotherapy, Chengdu, China

[8]State Key Laboratory of Pharmaceutical Biotechnology, Department of Hepatopancreatobiliary Surgery, Nanjing Drum Tower Hospital, The Affiliated Hospital of Nanjing University Medical School, MOE Key Laboratory of Model Animal for Disease Study, Model Animal Research Centre, Nanjing University, Nanjing, China

[9]Liverpool Pancreatitis Research Group, Liverpool University Hospitals NHS Foundation Trust and Institute of Translational Medicine, University of Liverpool, Liverpool, UK

Correspondence
Guotao Lu, Pancreatic Center, Department of Gastroenterology, Affiliated Hospital of Yangzhou University, Yangzhou University, 11 Huaihai Road, Yangzhou 225000, China.
Email: pkulgt@163.com

Weiqin Li, Center of Severe Acute Pancreatitis (CASP), Department of Critical Care Medicine, Jinling Hospital, Medical School of Nanjing University, 305 Zhongshan East Road, Nanjing 210002, China.
Email: njzy_pancrea@163.com

Funding information
Jiangsu Provincial Key Research and Development Program, Grant/Award Numbers: BE2015685, BE2016749; National Natural Science Foundation of China, Grant/Award Numbers: 81570584, 81670588, 81800575, 81801970, 81973632

Background and Purpose: Pyroptosis is a lytic form of pro-inflammatory cell death characterised as caspase 1 dependent with canonical NLRP3 inflammasome-induced gasdermin D (GSDMD) activation. We aimed to investigate the role of acinar pyroptotic cell death in pancreatic injury and systemic inflammation in AP.

Experimental Approach: Pancreatic acinar pyroptotic cell death pathway activation upon pancreatic toxin stimulation *in vitro* and *in vivo* was investigated. Effects of pharmacological (NLRP3 and caspase-1 inhibitors), constitutive (*Nlrp3*$^{-/-}$, *Casp1*$^{-/-}$ and *Gsdmd*$^{-/-}$) and acinar cell conditional (*Pdx1*^{Cre}*Nlrp3*$^{\Delta/\Delta}$ and *Pdx1*^{Cre}*Gsdmd*$^{\Delta/\Delta}$) genetic inhibition on pyroptotic acinar cell death, pancreatic necrosis and systemic inflammation were assessed using mouse AP models (caerulein, sodium taurocholate and L-arginine). Effects of *Pdx1*^{Cre}*Gsdmd*$^{\Delta/\Delta}$ versus myeloid conditional knockout (*Lyz2*^{Cre}*Gsdmd*$^{\Delta/\Delta}$) and *Gsdmd*$^{-/-}$ versus receptor-interacting protein 3 (RIP3) inhibitor were compared in CER-AP.

Abbreviations: AP, acute pancreatitis; ARG-AP, L-arginine induced AP; ASC, adaptor molecule apoptosis-associated speck-like protein with a caspase recruitment domain; CCK, cholecystokinin; CER-AP, caerulein induced AP; GSDMD, gasdermin D; H&E, haematoxylin and eosin; MLKL, mixed lineage kinase domain-like protein; NLRP3, NOD-1, LRR- and pyrin domain-containing 3; NaTC-AP, sodium taurocholate induced AP; PI, propidium iodide; RIPK1 and RIPK3, receptor-interacting serine/threonine protein kinase 1 and 3; WT, wild-type.

Lin Gao and Xiaowu Dong contributed equally to this manuscript.

Key Results: There was consistent pyroptotic acinar cell death upon pancreatic toxin stimulation both *in vitro* and *in vivo*, which was significantly reduced by pharmacological or genetic pyroptosis inhibition. *Pdx1*^{Cre}*Gsdmd*$^{\Delta/\Delta}$ *but not Lyz2*^{Cre}*Gsdmd*$^{\Delta/\Delta}$ *mice showed significantly reduced pyroptotic acinar cell death*, pancreatic necrosis and systemic inflammation in caerulein-AP. Co-application of RIP3 inhibitor on *Gsdmd*$^{-/-}$ mice further increased protection on caerulein-AP.

Conclusion and Implications: This work demonstrates a critical role for NLRP3 inflammasome and GSDMD activation-mediated pyroptosis in acinar cells, linking pancreatic necrosis and systemic inflammation in AP. Targeting pyroptosis signalling pathways holds promise for specific AP therapy.

KEYWORDS
acinar cell death, acute pancreatitis, gasdermin D, NLRP3 inflammasome, pyroptosis

1 | INTRODUCTION

AP is one of the commonest digestive diseases with an increasing global incidence (Petrov & Yadav, 2019), causing significant mortality, morbidity, reduced quality of life and socio-economic burden (Machicado et al., 2017). Severe AP is characterised by persistent organ failure, often accompanied with pancreatic necrosis and infection, with a mortality of 36–50% (Banks et al., 2013). Results from randomised clinical trials of pharmacological therapies for AP have been disappointing, without significant reduction of organ failure and/or mortality (Moggia et al., 2017; van Dijk et al., 2017). Recent evidence from large cohort studies has defined an early peak in both organ failure and mortality in severe AP (Schepers et al., 2019; Shi et al., 2019), highlighting a potentially critical interventional window of early cellular events (Lee & Papachristou, 2019). In support of this view, we found that early treatment had a much better effect than delayed in both experimental (Wen et al., 2015) and human AP (Zhang et al., 2019).

Two forms of pancreatic acinar cell death have long been recognised: apoptosis and necrosis. Apoptosis in experimental AP appears largely protective (Criddle et al., 2007), with the extent of apoptosis inversely correlated with necrosis and severity in multiple murine AP models (Kaiser et al., 1995). Since then, the role of different modes of acinar cell death in the severity of AP has been extensively investigated, including autophagic cell death (Gukovskaya et al., 2017), mitochondrial permeability transition-mediated regulated necrosis (Mukherjee et al., 2016) and necroptosis (Louhimo et al., 2016). Necroptosis is a caspase-independent form of necrotic cell death and is finely regulated by a set of intracellular signal pathways, including receptor-interacting serine/threonine protein kinase 1 and 3 (**RIPK1** and **RIPK3**), as well as **mixed lineage kinase domain-like protein (MLKL)** (Pasparakis & Vandenabeele, 2015). Crucially, inhibition of necroptosis (*Rip3* or *Mlkl* gene deletion or inhibitors) could only exert partial protective effects on acinar cells (Louhimo et al., 2016; Wu et al., 2013), suggesting that other forms of cell death may contribute to acinar cell injury in AP.

What is already known

- Acinar cell necrosis drives the inflammatory response in AP.
- The role of pyroptotic acinar cell death in AP is unclear.

What does this study add

- A comprehensive study of the role of acinar cell pyroptosis in AP to date.
- Genetic and pharmacological pyroptosis inhibition reduced pyroptotic acinar cell death, pancreatic necrosis and systemic inflammation.

What is the clinical significance

- Pyroptosis in AP contributes to both local and systemic inflammatory response.
- These findings support the development of drugs that target pyroptosis inhibition for AP.

Pyroptosis is a caspase-dependent (caspases 1 and 11 for mice; caspases 1, 4 and 5 for human) and highly immunogenic form of cell death, characterised by release of pro-inflammatory cytokines and cellular contents (Linkermann et al., 2014). Pyroptosis plays a pivotal role in sepsis, ischaemia and type 2 diabetes mellitus (Guo et al., 2015) and is mainly regulated by the canonical **NOD-1, LRR- and pyrin domain-containing 3 (NLRP3)** inflammasome pathway (Schroder & Tschopp, 2010). Upon sensing a danger signal, the inflammasome recruits an adaptor molecule apoptosis-associated speck-like protein with a caspase recruitment domain (ASC) and an effector, cysteine protease **caspase 1**, to form the NLRP3 inflammasome complex. Active

caspase 1 has two major functions within the cells:- first, to convert pro-IL-1β into its bioactive form that promotes inflammation and second, to cleave gasdermin D (GSDMD), the final and direct executor of pyroptotic cell death, to release a 22-kDa C-terminal fragment and a 31-kDa N-terminal fragment (Kayagaki et al., 2015; Shi et al., 2015). The N-terminal fragment then moves to the plasma membrane, there binding to phosphoinositide and cardiolipin, leading to pore formation (10–14 nm) that allows release of mature **IL-1β** and **IL-18** (Ding et al., 2016).

The study of pyroptosis in AP is a novel undertaking. The aim of this study was to understand the role of pyroptosis in AP using genetic and pharmacological inhibition of key pyroptotic pathway components. Conditional acinar cell and myeloid-specific knockout mice were used to assess the importance of acinar cell-specific pyroptosis, with necroptosis inhibitors to assess the relative impact of these different modes of cell death.

2 | METHODS

2.1 | Ethics

The Principles of Laboratory Animal Care (NIH Publication No. 85Y23, revised 1996) were followed, and the study protocol was approved by the Ethics Committee of Jinling Hospital, Medical School of Nanjing University (No. 20160905). Human pancreatic sample collection was approved by the Human Ethics Committee of Jinling Hospital (No. 2018NZKY-009-01) and the study was conducted in accordance with the principles of Good Clinical Practice and the Declaration of Helsinki. Informed consents were obtained from all participants from whom pancreatic samples were procured.

2.2 | Materials

Cholecystokinin (C2175), **lipopolysaccharide (LPS)** (L2630), sodium taurocholate (T4009), caerulein (C9026), DMSO (D2650), BSA (B2064), anti-GAPDH primary antibody (G9545, RRID:AB_796208), the secondary goat anti-rabbit (AP132P, RRID:AB_90264) and goat anti-mouse (AP124P, RRID:AB_90456) IgG HRP antibodies were from Sigma-Aldrich (St. Louis, MO, USA). The NLRP3 inhibitor **MCC950** (HY-12815), caspase-1 inhibitor **VX-765 (beinacasin)** (HY-13205) and the RIP3 inhibitor GSK872 (HY-101872) were from MedChem Express (Monmouth Junction, NJ, USA). Caspase-1 inhibitor **Z-YVAD-FMK** was from APExBio (Houston, TX, USA). Anti-NLRP3 antibody (15101, RRID:AB_2722591) was from Cell Signaling Technology (Danvers, MA, USA). Anti-caspase 1 (sc-56036, RRID:AB_781816) and anti-GSDMD (sc-81868, RRID:AB_2263768) were from Santa Cruz Biotechnology (Dallas, TX, USA). Anti-GSDMD (ab-219800, RRID:AB_2888940), anti-β-actin (ab-8227, RRID:AB_2305186), anti-amylase (ab-21156, RRID:AB_446061) antibodies and anti-rabbit IgG H&L (Alexa Fluor 488) (ab150073, RRID:AB_2636877) were from Abcam (Cambridge, UK). Lipofectamine 3000 (L3000015) was from Invitrogen (Carlsbad, CA, USA). FAM-FLICA Caspase-1 Assay Kit (9146) was from ImmunoChemistry Technologies (Bloomington, MN, USA). Mouse IL-1β ELISA Kit (MLB00C) was from R&D Systems (Minneapolis, MN, USA). Mouse IL-6 (BMS603-2), TNF-α ELISA kits (BMS607-3) and BCA protein assays were from Thermo Fisher Scientific (Shanghai, China). Calcein-AM (C326), LDH Cytotoxicity Assay Kit (CK12) and Cell Counting Kit (CK04) were from Dojindo (Kumamoto, Japan). Serum amylase kit was from Biosino Biotechnology (Beijing, China), and lipase kit was from Nanjing Jiancheng Corp. (Nanjing, China). Antibodies used for flow cytometry, CD45 (clone 104), CD11b (clone M1/70), F4/80 (clone BM8) and TNF-α (clone MP6-XT22) were from BioLegend (San Diego, CA, USA).

2.3 | Human pancreas collection

Normal human pancreatic tissues were procured from patients who underwent Whipple's surgery or distal pancreatectomy for the indication of pancreatic malignancy. In view of the difficulty in getting pancreatic tissues from patients with AP, tissues of chronic pancreatitis were obtained from patients who received therapeutic surgical procedures instead. Briefly, a 2- to 4-cm^3-sized pancreatic tissue was cut and immediately washed twice with PBS. Then it was transferred into 4% paraformaldehyde for preparation of formalin-fixed paraffin-embedded specimen.

2.4 | Animals

Eight-week male wild-type (WT) and genetic knockout mice were from the Model Animal Research Centre of Nanjing University (*Casp1*$^{-/-}$ and *Gsdmd*$^{-/-}$) or Nanjing Medical University (*Nlrp3*$^{-/-}$). *Pdx1*^{Cre} (IMSR Cat# JAX:014647, RRID:IMSR_JAX:014647) and *Lyz2*^{Cre} (IMSR Cat# JAX:004781, RRID:IMSR_JAX:004781) mice were from The Jackson Laboratory (Bar Harbor, ME, USA). Pancreatic acinar cell *Nlrp3* and *Gsdmd* specific knockout (*Pdx1*^{Cre}*Nlrp3*$^{\Delta/\Delta}$ and *Pdx1*^{Cre}*Gsdmd*$^{\Delta/\Delta}$) mice were generated by intercrossing *Pdx1*^{Cre} mice with *Nlrp3*$^{flox/flox}$ and *Gsdmd*$^{flox/flox}$ mice, respectively. Myeloid cell GSDMD specific knockout (*Lyz2*^{Cre}*Gsdmd*$^{f/f}$) mice were generated by intercrossing *Lyz2*^{Cre} mice with *Gsdmd*$^{flox/flox}$ mice. All mice were of C57BL/6 background. All mice were housed under specific pathogen-free (SPF) conditions in individually ventilated cages with wood pieces as bedding material (3–5 mice per cage) at 24°C on a 12-h dark/light cycle. Animals were allowed access to water and standard laboratory chow *ad libitum*. All animal studies are reported in compliance with the ARRIVE guidelines (Percie du Sert et al., 2020) and with the recommendations made by the *British Journal of Pharmacology* (Lilley et al., 2020).

2.5 | Randomisation, blinding and sample size estimation

Mice were marked with earmark, and randomised table was used. Mice were divided into groups in completely randomised design

manner. The animal groupings were blinded to the pathologists but not to the experiment operators.

Based on our preliminary experiments, the usual values of cell death area in pancreatic tissues from CER-AP mice are ~20% with SD of ~6%. We want to be able to detect from the treatment/gene modification a meaningful 50% reduction from diseased control levels while assuming an alpha 0.05 and 80% power, this requires group size ~6 mice per group (sample size calculator: https://clincalc.com/Stats/SampleSize.aspx).

2.6 | Induction of AP and administration of pyroptosis inhibitors

Three different AP models were used: (i) caerulein (200 $\mu g \cdot kg^{-1}$), a **cholecystokinin (CCK)** analog, was intraperitoneally injected at an hour interval for 10 times to induce hyperstimulation AP (CER-AP), whereas controls received PBS injections (Liu et al., 2018); (ii) Sodium taurocholate was infused retrogradely into the pancreatic duct to induce biliary acute pancreatitis. Briefly, a combination of nembutal and buprenorphine was used as the anesthetic/analgesic agents. The mouse was allowed to breath spontaneously and no intubation/ventilation was used. 2.5% **sodium taurocholate** was infused retrogradely into the pancreatic duct (with a clamp across the upper end at the liver hilum) at a speed of 5 $\mu l \cdot min^{-1}$ for 10 min by minipump (Harvard Apparatus, Kent, UK) to induce biliary acute pancreatitis, whereas controls underwent the same procedure without **sodium taurocholate** infusion. After the procedures, the mouse was returned to its cage placed on a heated pad (37 °C) until it recovered (Perides et al., 2010) and (iii) **L-arginine** (8%, 3 $g \cdot kg^{-1}$; pH 7.4) was intraperitoneally administered hourly for three times to induce excessive amino acid-induced AP (ARG-AP) and controls received PBS injections (Kui et al., 2015).

In the treatment groups for CER-AP and NaTC-AP, specific inhibitors for NLRP3 (MCC950; 50 $mg \cdot kg^{-1}$) (Coll et al., 2015) and caspase 1 (beinacasin/VX-765; 200 $mg \cdot kg^{-1}$) (McKenzie et al., 2018) were intraperitoneally injected immediately before (prophylactically) and 1 h after (therapeutically) AP induction, respectively. RIP3 inhibitor (GSK872; 5 $mg \cdot kg^{-1}$) (Mandal et al., 2014) was intraperitoneally injected to observe the effects of necroptosis inhibition on AP. If not specified, mice in CER-AP, NaTC-AP and excessive ARG-AP and their control groups were humanely killed at 12, 24 and 72 h after AP induction, respectively.

2.7 | Isolation of pancreatic acinar cells, cell culture and transfection

Pancreatic acinar cells were freshly isolated from mice using a collagenase digestion procedure as previously described (Huang et al., 2017). Mouse pancreatic acinar carcinoma 266-6 cells were obtained from American Type Culture Collection (ATCC Cat# CRL-2151, RRID: CVCL_3481) and cultured in DMEM supplemented with 10% FBS, 100-$U \cdot m^{-1}$ penicillin and 100-$\mu g \cdot m^{-1}$ streptomycin. For siRNA transfection, 266-6 cells were transfected with 150-$nmol \cdot L^{-1}$ GSDMD siRNA oligonucleotides for 24 h using Lipofectamine 3000 according to the manufacturer's protocol. Transfected cells were incubated with CCK (8 μM) or sodium taurocholate (1 mM) for 12 h after transfection. Knock-down efficacy was assessed by western blot analysis. The GSDMD siRNA sequence used for transfections is listed in Table S1.

2.8 | Acinar cell death assays

Pyroptotic cell death in 266-6 cells was detected by double staining of activated caspase 1 (FAM-FLICA Caspase-1 Assay Kit; dilution 1:50) and propidium iodide (PI) (4 μM) according to the manufacturer's instruction. Stained cells were then analysed by ACEA Novocyte flow cytometry (ACEA Biosciences Inc., San Diego, CA, USA). Necrotic cell death was determined by PI (4 μM; for dying/dead cells) and calcein-AM (2 μM; for living cells) and visualised with an Olympus Research Inverted System Microscope IX71 (Olympus, Tokyo, Japan). Cell death was also expressed as lactic dehydrogenase (LDH) release in the cell culture supernatant and assessed using a LDH Cytotoxicity Assay Kit. Viable cells were determined by a Cell Counting Kit.

2.9 | Isolation of leukocytes and flow cytometry

The leukocytes in pancreas were isolated using a collagenase digestion method described for flow cytometry analysis (Xue et al., 2012). For surface staining, immune cells were stained with the following antibodies: Alexa Fluor 700-conjugated CD45.2, APC-conjugated CD11b, Pacific Blue-conjugated F4/80 and PE-conjugated TNF-α. Pro-inflammatory macrophages (M1 phenotype) were gated as $(CD45.2^{+})/(CD11b^{+})/(F4/80^{+})/(TNF\text{-}\alpha^{+})$ in flow cytometry. Flow cytometry data collection was performed on FACS Aria II flow cytometer (BD Inc., Franklin Lakes, NJ, USA) and analysed using FlowJo software (RRID:SCR_008520).

2.10 | AP severity assessment

2.10.1 | Histopathological examination

The paraffin sections of pancreatic and lung tissue were stained with haematoxylin and eosin (H&E). Pancreatic acinar cell death was defined as a decrease in basophilic acinar cytoplasm or vacuolar degeneration in cytoplasm, and formation of dense nuclei. Cell death area was semi-quantified by two independent observers who were unaware of the experimental design and grouping. It was then calculated as cell death area divided by total pancreatic parenchyma × 100% by using ImageJ 1.50 software (National Institutes of Health, USA, RRID:SCR_003070). The degree of lung injury was evaluated by the severity of

neutrophil infiltration, thickness of alveolar and alveolar congestion and the scoring standards were described previously (Pan et al., 2017).

2.10.2 | Serum amylase, lipase and pro-inflammatory cytokines

Serum amylase and lipase levels were determined by respective commercial kits; serum cytokines, IL-1β, IL-6 and TNF-α were measured using ELISA kits according to the manufacturer's protocols.

2.11 | Western blotting

Western blotting analysis was performed on whole-cell extracts and pancreatic tissues. Total amounts of protein were quantified by BCA protein assay according to the manufacturer's protocol. According to our previously described methods (Gao et al., 2018), the membranes were incubated overnight at 4°C with primary antibodies against NLRP3 (1:1000 dilution), caspase 1 (1:500 dilution), GSDMD (1:500 dilution), β-actin (1:2000 dilution) or GAPDH (1:4000 dilution) in blocking buffer. On the next day, membranes were washed with Tris-buffered saline with Tween 20 (TBST; 3 × 10 min) and incubated with a secondary IgG HRP antibody (1:10,000 dilution) diluted in 5% (w/v) dry non-fat milk in TBST for 2 h at room temperature. Finally, membranes were washed with TBST (3 × 10 min) and all blots were developed by using the ECL Plus chemiluminescent system. The Immuno-related procedures used comply with the recommendations made by the *British Journal of Pharmacology* (Alexander et al., 2018).

2.12 | Immunofluorescence

Briefly, slices were prepared and blocked with 5% BSA in PBST (PBS containing 0.05% Tween 20) for 0.5 h. Slices were then incubated with anti-GSDMD (1:200 dilution) and anti-amylase (1:200 dilution) antibodies overnight at 4°C, and Alexa Fluor 488 (green)-labelled anti-rabbit IgGs were then loaded for 2 h at room temperature in the dark. After washing, DAPI was used for nuclear staining. Stained specimens were visualised with an Olympus Research Inverted System Microscope IX71 (Olympus, Tokyo, Japan).

2.13 | Transmission electron microscope

Briefly, fresh tissue blocks are isolated preventing from physical damage, with size of tissue block no more than 1 mm^3. Put the tissue blocks in fixative at 4°C for 2–4 h. Wash in 0.1-M PBS for three times, 15 min each; postfix with 1% OsO_4 in 0.1-M PBS (pH 7.4) for 2 h at room temperature. Remove OsO_4 and rinse in 0.1-M PBS (pH 7.4) for three times, 15 min each. Dehydrate as follows: 50% ethanol for 15 min; 70% ethanol for 15 min; 80% ethanol for 15 min; 90% ethanol for 15 min; 95% ethanol for 15 min; two changes of 100% ethanol for 15 min; and finally, two changes of acetone for 15 min. Infiltrate 1:1 acetone:EMbed 812 for 2–4 h; 2:1 acetone:EMbed 812 overnight in desiccator with top off; and pure EMbed 812 for 5–8 h; keep in 37°C oven overnight; and embed by baking in 60°C oven for 48 h. Cut ultrathin sections (60–80 nm) with ultramicrotome. Stain sections with uranyl acetate in pure ethanol for 15 min and rinse with distilled water. Then stain with lead citrate for 15 min and rinse with distilled water. Allow sections air dry overnight. Observe with transmission electron microscope (Hitachi, HT7700).

2.14 | Statistical analysis

The data and statistical analysis comply with the recommendations of the *British Journal of Pharmacology* on experimental design and analysis in pharmacology (Curtis et al., 2018). Statistical analysis was undertaken only for studies where each group size was at least $n = 5$. The declared group size is the number of independent values, and the statistical analysis was done using these independent values. Results are presented as the mean ± SEM in scatter plots. The distribution of data was assessed by Kolmogorov–Smirnov test. If data follow Gaussian distribution, parametric tests (Student's *t*-test for comparison between two groups or one-way ANOVA for three or more groups) were carried out. For ANOVA, Bonferroni posttest was performed for data with *F* at $P < .05$ and no significant variance in homogeneity. If data were not normally distributed, non-parametric tests (Mann–Whitney *U*-test for two groups or Kruskal–Wallis test with Dunns' posttest for three or more groups) were used. Data were analysed using GraphPad Prism software (Version 6.0, GraphPad Software Inc., San Diego, CA, USA, RRID:SCR_002798) and IBM SPSS Statistics 22.0 (IBM Corporation, Armonk, NY, USA). A two-sided *p* value of <.05 was considered to be statistically significant.

2.15 | Nomenclature of targets and ligands

Key protein targets and ligands in this article are hyperlinked to corresponding entries in the IUPHAR/BPS Guide to PHARMACOLOGY http://www.guidetopharmacology.org and are permanently archived in the Concise Guide to PHARMACOLOGY 2019/20 (Alexander et al., 2019).

3 | RESULTS

3.1 | Pancreatic toxins induce pyroptotic cell death in pancreatic acinar cells

We first examined whether the classic pancreatic toxins CCK and sodium taurocholate cause pyroptosis in freshly isolated mouse

pancreatic acinar cells and cultured 266-6 cells (Talukdar et al., 2016; Zhou et al., 2015), a mouse pancreatic acinar carcinoma cell line retaining key acinar cell characteristics and displaying similar responses on exposure to extracellular danger signals. The pyroptosis activation-associated proteins,NLRP3, GSDMD and caspase 1, were detected by western blot. Specifically, GSDMD and cleaved GSDMD, caspase 1 and cleaved caspase 1 were exposed on an Immobilon-NC membrane together using protocols by previous studies (Li et al., 2020; Ma et al., 2020). LPS priming followed by nigericin treatment, commonly used in a range of cell types but never assessed in pancreatic acinar cells before, was used to induce pyroptotic cell death pathway activation (Chang et al., 2018; He et al., 2015). Double-positive staining of caspase 1/PI in flow cytometry was used to detect the presence of pyroptosis in *in vitro* experiments.

CCK induced NLRP3, caspase 1 and GSDMD activation, as evidenced by up-regulation of NLRP3, cleaved caspase 1 and cleaved GSDMD proteins in both freshly isolated mouse pancreatic acinar cells and cultured 266-6 cells (Figure 1a). In 266-6 cells, nigericin and LPS caused significant and dramatic increase of pyroptotic cells, compared with PBS alone (35.4 ± 1.0% vs. 2.8 ± 0.2%). Both CCK ([8 μM] 14.2 ± 0.3% vs. [4 μM] 10.6 ± 0.4% vs. [2 μM] 6.9 ± 0.3%; vs. [PBS] 1.1 ± 0.4%) and sodium taurocholate ([1 mM] 11.5 ± 0.7% vs. [0.75 mM] 8.8 ± 0.5% vs. [0.5 mM] 5.3 ± 0.3% vs. [PBS] 0.7 ± 0.4%) dose-dependently significantly induced pyroptotic cell death in 266-6 cells (Figure 1b).

The transmission electron microscope was further used to observe the morphological features of the pyroptotic cells. Compared with the PBS control, there were marked nuclear membrane rupture, nuclear chromatin condensation, and dilated mitochondria and endoplasmic reticulum in pancreatic acinar cells in CER-AP mice (Figure 1c).

3.2 | GSDMD is activated in mouse AP models and human pancreatitis

Both repeated caerulein intraperitoneal injections and pancreatic ductal retrograde sodium taurocholate perfusion caused typical pathological changes of marked pancreatic oedema, diffused parenchymal inflammatory cell infiltration and acinar cell necrosis (Figure 2a). The pancreatic necrosis peaked at 12 h in CER-AP and remained high at 24 h, whereas in NaTC-AP, pancreatic necrosis was maximal at 24 h and remained high at 72 h. Western blot analyses revealed significant up-regulation of NLRP3, cleaved caspase 1 and cleaved GSDMD proteins in pancreatic tissues from both CER-AP and NaTC-AP at various time points (Figure 2b). In both AP mouse models and human chronic pancreatitis, the pancreas had a high density of anti-GSDMD immunofluorescence, predominately within acinar cells compared with respective controls (Figure 2c).

3.3 | Pyroptosis inhibition reduces acinar cell death *in vitro* as well as pancreatic necrosis and systemic inflammation *in vivo*

Selective NLRP3 inhibitor (MCC950) and selective caspase-1 inhibitor (Z-YVAD-FMK) separately reduced CCK- and sodium taurocholate-induced cell death significantly in freshly isolated acinar cells and 266-6 cells, demonstrated as reduced PI-positive cells in Calcein-PI staining (Figure 3a, Calcein-AM for living cells and PI for dead/dying cells) as well as reduced LDH release and promoted cell survival (Figure 3b,d). Of note, these inhibitors significantly mitigated both CCK- and sodium taurocholate-induced pyroptotic cell death in 266-6 cells shown by flow cytometry (Figure 3c). In agreement with the above findings, freshly isolated pancreatic acinar cells from *Gsdmd*$^{-/-}$ mice showed significantly reduced cell death in Calcein-PI staining (Figure 4a) and LDH release that was inversely mirrored by surviving cells (Figure 4b) after CCK or sodium taurocholate incubation. Knock-down of GSDMD (using GSDMD siRNA) compared with scrambled siRNA in 266-6 cells also significantly attenuated CCK- and sodium taurocholate-induced pyroptotic cell death and LDH release and promoted cell survival (Figure 4c,d).

Specific NLRP3 inhibitor (MCC950) and caspase-1 inhibitor (VX-765) mitigated pancreatic injury and systemic inflammation as reflected by significantly reduced pancreatic acinar cell death percentage, severity of acute lung injury (Figure 5a), and serum IL-1β, IL-6 and TNF-α levels (Figure 5b) compared with caerulein alone. The similar protective effects of MCC950 and VX-765 were shown in NaTC-AP model (Figure S1). Neither inhibitor altered serum amylase or lipase levels in both AP models. In order to explore the therapeutic effect of NLRP3 inflammasome component inhibitors, MCC950 and VX-765 were administrated 1 h after CER-AP induction. Similarly, the protective effects on pancreatic injury and systemic inflammation were shown, but serum amylase or lipase levels still remained unaffected (Figure S2).

Genetic deletion of *Nlrp3* or *Casp1* also significantly reduced pancreatic acinar cell death percentages, severity of acute lung injury, serum amylase and lipase, and serum IL-1β, IL-6 and TNF-α levels in CER-AP (Figure 6a,b). These findings were consistent with a previous published study (Hoque et al., 2011). Western blotting analyses demonstrated that NLRP3 or caspase-1 deletion down-regulated caerulein-induced activation of NLRP3, cleaved caspase 1 and cleaved GSDMD compared with their respective WT littermates (Figure 6c). Furthermore, *Gsdmd* genetic deletion significantly reduced pancreatic acinar cell death percentages, severity of acute lung injury (Figure 7a), serum amylase, lipase, and IL-1β, IL-6 and TNF-α levels (Figure 7b) compared with WT littermates in CER-AP. Pancreatic acinar cell death percentages, serum amylase, lipase and IL-1β levels were also significantly reduced in *Gsdmd*$^{-/-}$ mice in both NaTC-AP and ARG-AP (Figure 7a,b). Western blotting results of pancreatic tissues from CER-AP and NaTC-AP indicated that activation of NLRP3, cleaved caspase 1 and cleaved GSDMD was suppressed in *Gsdmd*$^{-/-}$ mice (Figure 7c).

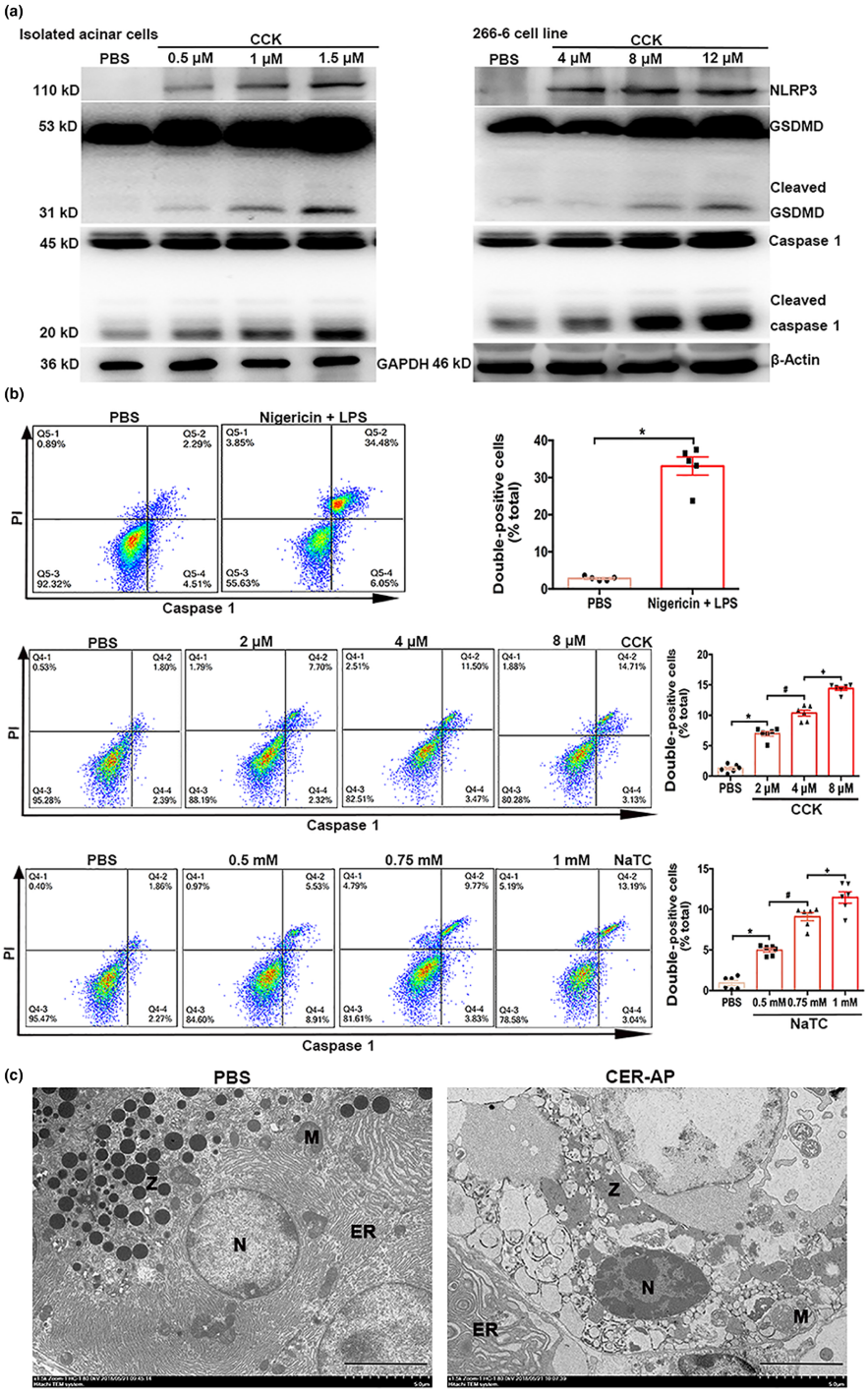

FIGURE 1 Pancreatic toxins induce pyroptosis in mouse pancreatic acinar cells. (a) Cholecystokinin (CCK) induced activation of caspase 1, NLRP3 and gasdermin D (GSDMD) in (i) freshly isolated pancreatic acinar cells and (ii) pancreatic acinar carcinoma 266-6 cells. $N = 5$ per group. (b) Pyroptotic 266-6 cells identified using double staining of caspase 1 (dilution 1:50) and propidium iodide (PI; 4 μM) and observed using flow cytometry: (i) cells were incubated with LPS (400 $ng \cdot m^{-1}$) for 4 h followed by nigericin (20 μM) for 2 h, positive inducer for pyroptosis. Data were expressed as mean ± SEM, $n = 5$ per group, $^{*}p < .05$ versus PBS. (ii) Cells were incubated with CCK for 12 h. Data were expressed as mean ± SEM, $n = 6$ per group, $^{*}P < .05$ versus PBS, $^{\#}P < .05$ versus CCK 2 μM and $^{+}P < .05$ versus CCK 4 μM. (iii) Cells were incubated with sodium taurocholate (NaTC) for 12 h. Data were expressed as mean ± SEM, $n = 6$ per group, $^{*}p < 0.05$ versus PBS, $^{\#}p < 0.05$ versus NaTC 0.5 mM, $^{+}p < 0.05$ versus NaTC 0.75 mM. (c) Morphological features of pyroptotic acinar cells observed by transmission electron microscope. Mice received 10 intraperitoneal injections of caerulein (CER) at hourly interval to induce acute pancreatitis (AP) or PBS served as control and were killed 12 h after the first PBS/CER injection. Left: electron micrograph of a normal pancreatic acinar cell showing normal nucleus (N), mitochondria (M), zymogen granules (Z) and endoplasmic reticulum (ER). Right: electron micrograph of the pancreatic acinar cell from caerulein-induced acute pancreatitis (CER-AP) mice showing a nucleus (N) with peripheral condensation of chromatin, dilated mitochondria (M) and endoplasmic reticulum (ER). Scale bar, 5 μm. $n = 5$ per group

3.4 | Acinar cell-specific *Nlrp3* and *Gsdmd* knockout attenuates the severity of CER-AP

To confirm that the decrease of pancreatic necrosis in knockout mice was indeed attributable to the lack of NLRP3 and GSDMD expression in pancreatic acinar cells, we generated conditional pancreatic acinar cell-specific gene knockout mice. Both *Nlrp3* and *Gsdmd* conditional knockout mice were found to display significantly reduced pancreatic acinar cell death percentages, severity of acute lung injury (Figure 8a), reduced serum severity indices (Figure 8b) and down-regulation of pyroptosis-related proteins in pancreatic tissues (Figure 8c) in CER-AP compared with WT littermates.

Myeloid cell *Gsdmd* conditional knockout mice, however, displayed similar pro-inflammatory macrophage (M1) infiltration in pancreatic tissues after CER-AP induction when compared with their WT littermates. The pancreatic acinar cell death percentages, serum amylase and lipase levels were not significantly different between the two groups (Figure S3).

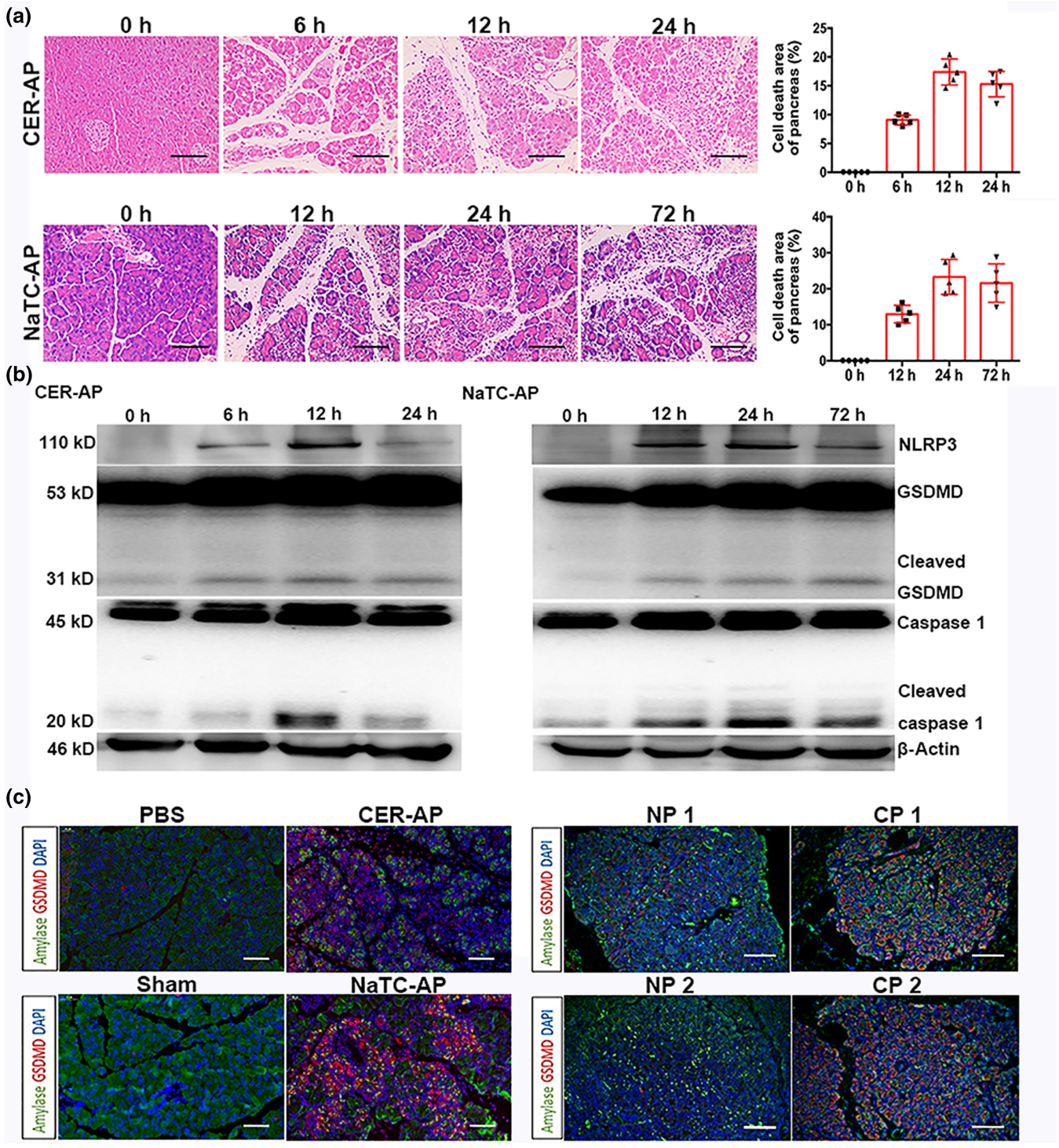

FIGURE 2 Pancreatic NLRP3 inflammasome and gasdermin D (GSDMD) activation in mouse acute pancreatitis (AP) models and human pancreatitis. Details for experimental AP induction and human sample collection were described in Section 2. Caerulein (CER) and sodium taurocholate (NaTC) were used to induce AP in mice. (a) Representative H&E images and pancreatic cell death percentages. Scale bar, 100 μm. Data were expressed as mean ± SEM, $n = 5$ per group. (b) Western blotting analysis of pyroptosis-related proteins in mouse pancreatic tissues. $N = 5$ per group. (c) Immunofluorescence GSDMD staining of pancreatic tissues from mice (PBS injection vs. caerulein-induced acute pancreatitis (CER-AP); sham surgery vs. sodium taurocholate-induced acute pancreatitis [NaTC-AP]) and human (normal pancreas [NP] vs. chronic pancreatitis [CP]). Scale bar, 100 μm. $n = 5$ per group

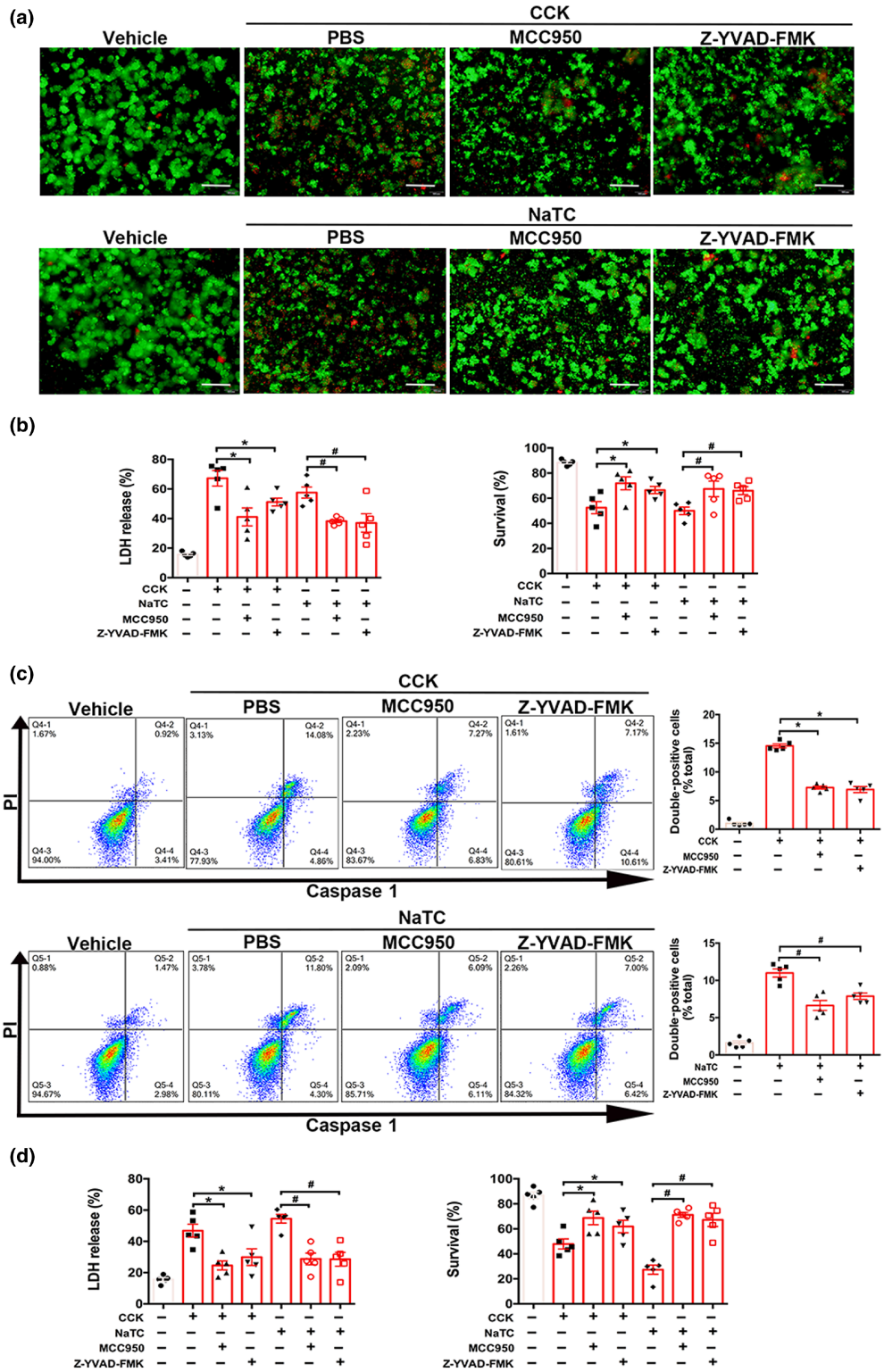

FIGURE 3 Pyroptosis inhibitors attenuate pancreatic acinar cell death. In these experiments, freshly isolated pancreatic acinar cells and 266-6 cells were incubated with 1- and 8-μM cholecystokinin (CCK) and 0.5- and 1-mM sodium taurocholate (NaTC), respectively, or PBS alone (vehicle), for 12 h. In the treatment groups, cells were co-incubated with selective NLRP3 inhibitor (MCC950; 20 nM) and selective caspase-1 inhibitor (Z-YVAD-FMK; 10 μM). (a) Representative living (calcein-AM; 2 μM) and dying/dead (propidium iodide [PI]; 4 μM) cell images from epifluorescence microscopy for acinar cells. Scale bar, 200 μm. $N = 5$ per group. (b) Cell death of acinar cells determined by LDH release and Cell Counting Kit. Data were expressed as mean ± SEM, $n = 5$ per group, $^{*}P < .05$ versus CCK and $^{\#}P < .05$ versus NaTC. (c) Pyroptotic 266-6 cells identified using double staining of caspase 1 (dilution 1:50) and PI (4 μM) and observed using flow cytometry. Data were expressed as mean ± SEM, $n = 5$ per group, $^{*}P < .05$ versus CCK and $^{\#}P < .05$ versus NaTC. (d) Cell death of 266-6 cells determined by LDH release and Cell Counting Kit. Data were expressed as mean ± SEM, $n = 5$ per group, $^{*}P < .05$ versus CCK and $^{\#}P < .05$ versus NaTC

3.5 | Necroptosis inhibition adds more protection to *Gsdmd* knockout mice in CER-AP

As necroptosis has been reported to be important in AP (Louhimo et al., 2016; Wu et al., 2013), we wondered whether GSDMD-mediated pyroptosis was an independent cell death pathway and distinct from necroptosis in pancreatic acinar cells. We added necroptosis inhibitor GSK872 into GSDMD knock-down 266-6 cells upon CCK stimulation. We found that GSDMD knock-down significantly reduced the percentage of PI-positive cells by 32%

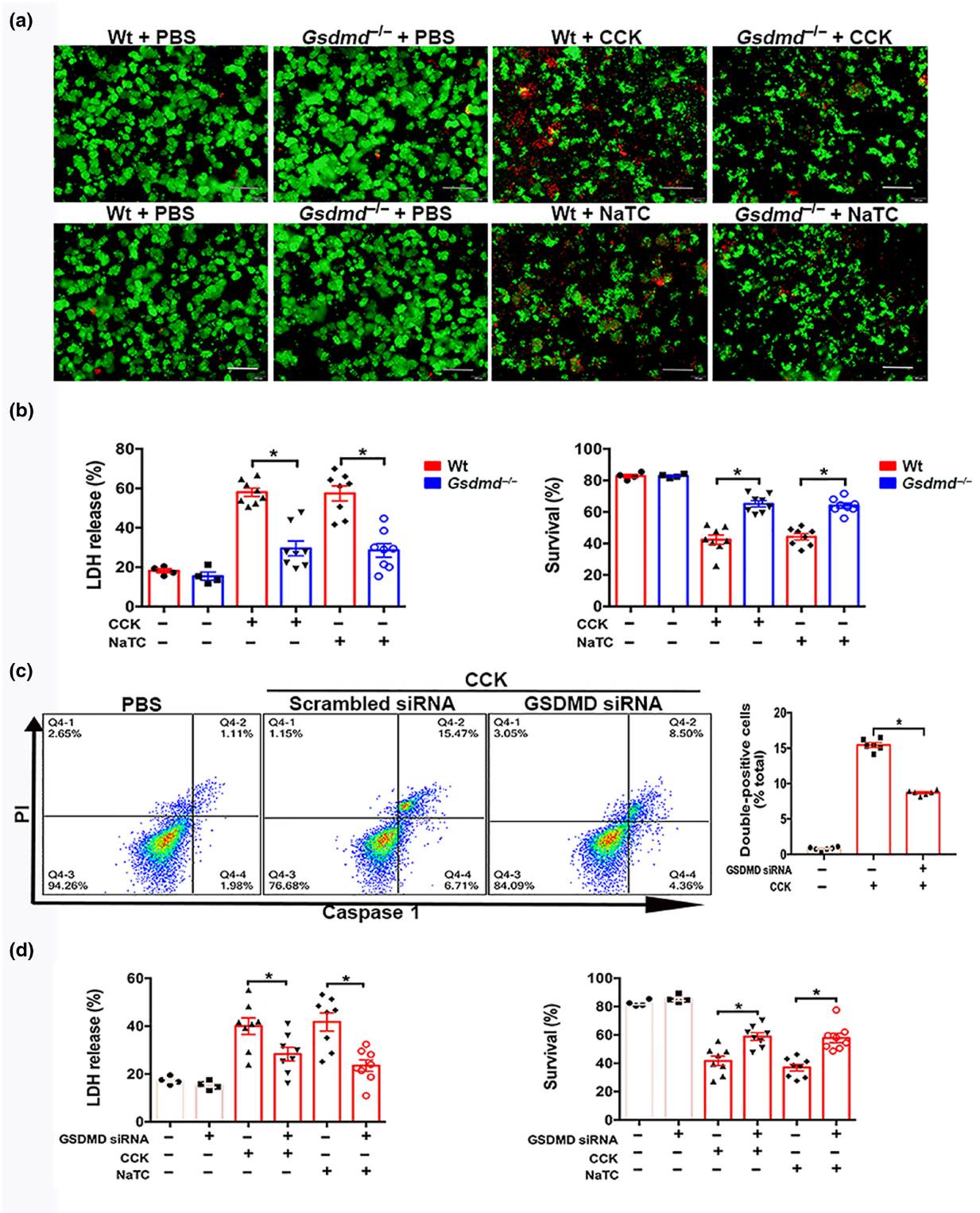

FIGURE 4 *Gsdmd* deficiency attenuates pancreatic acinar cell death. In these experiments, freshly isolated pancreatic acinar cells were incubated with cholecystokinin (CCK; 1 μM) or sodium taurocholate (NaTC; 0.5 mM), respectively, 266-6 cells were incubated with CCK (8 μM), or PBS alone, for 12 h. (a) Representative living (calcein-AM; 2 μM) and dying/dead (propidium iodide [PI]; 4 μM) cell images from epifluorescence microscopy for acinar cells from wild-type (WT) and *Gsdmd* knockout (*Gsdmd*$^{-/-}$) mice. Scale bar, 200 μm. $N = 5$ per group. (b) Cell death of acinar cells (WT or *Gsdmd*$^{-/-}$) determined by LDH release and Cell Counting Kit. Data were expressed as mean ± SEM, $n = 8$ per group, $^*P < .05$ versus WT. (c) Pyroptotic 266-6 cells (scrambled or gasdermin D [GSDMD] siRNA) identified using double staining of caspase 1 (dilution 1:50) and PI (4 μM) and observed using flow cytometry. Data were expressed as mean ± SEM, $n = 6$ per group, $^*P < .05$ versus scrambled siRNA. (d) Cell death of 266-6 cells (scrambled or GSDMD siRNA) determined by LDH release and Cell Counting Kit. Data were expressed as mean ± SEM, $n = 8$ per group, $^*P < .05$ versus scrambled siRNA

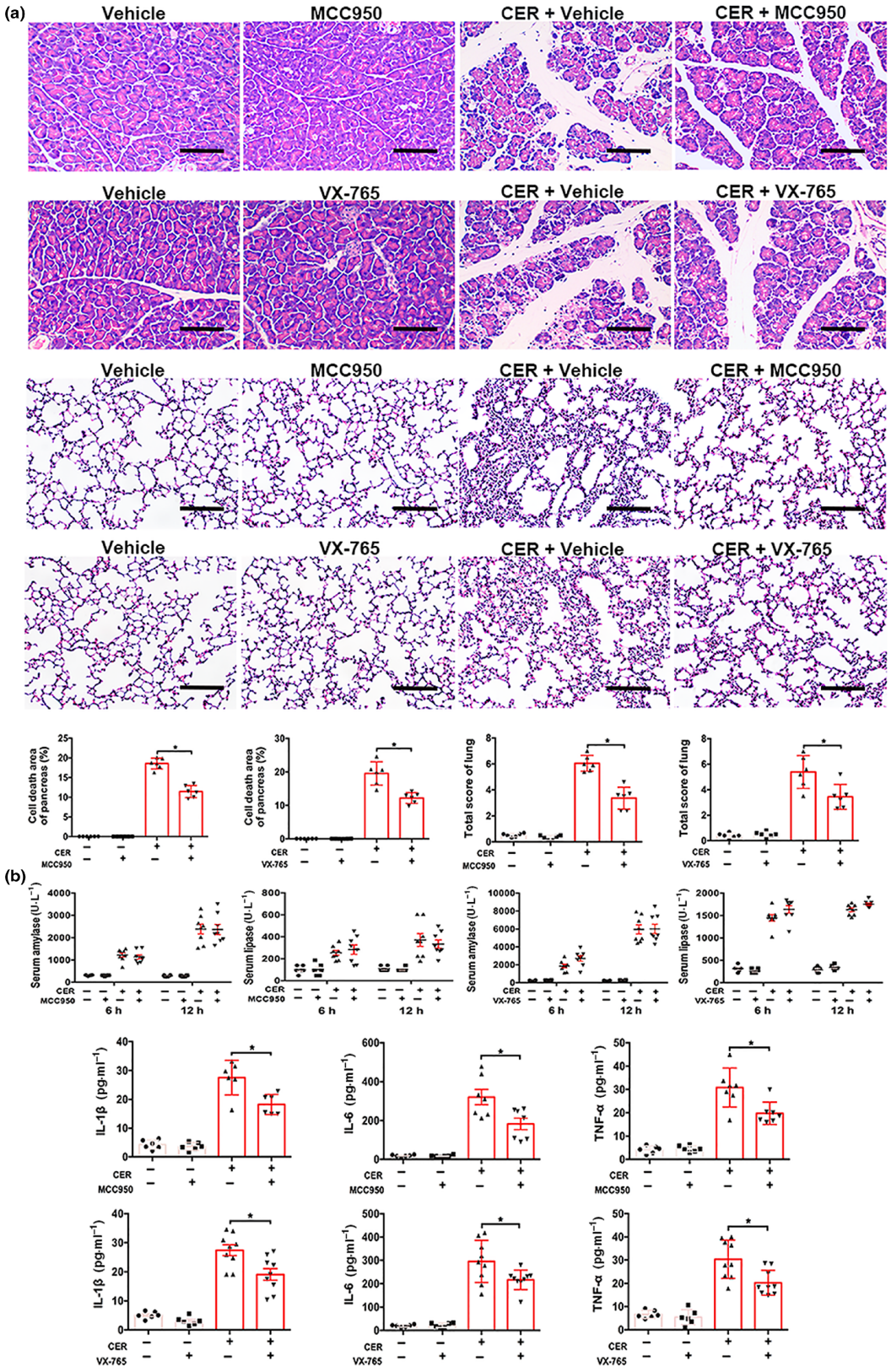

FIGURE 5 NLRP3 inhibitor (MCC950) and caspase-1 inhibitor (VX-765) mitigate pancreatic necrosis and systemic inflammation in caerulein-induced acute pancreatitis (CER-AP). Details for experimental AP induction and severity assessment were described in Section 2. In the treatment groups, mice received single intraperitoneal injection of MCC950 (50 mg·kg^{-1}) or VX-765 (200 mg·kg^{-1}) immediately before AP induction. Animals were killed at 12 h after the first CER/PBS injection. (a) Representative H&E images of pancreas, lung and pancreatic cell death percentages, and total histological scores of lung injury. Scale bar, 100 μm. Data were expressed as mean ± SEM, $n = 6$ per group, $^*P < .05$ versus CER. (b) Serum amylase, lipase, and IL-1β, IL-6 and TNF-α levels. Data were expressed as mean ± SEM, $n = 6$ per group, $^*P < .05$ versus CER

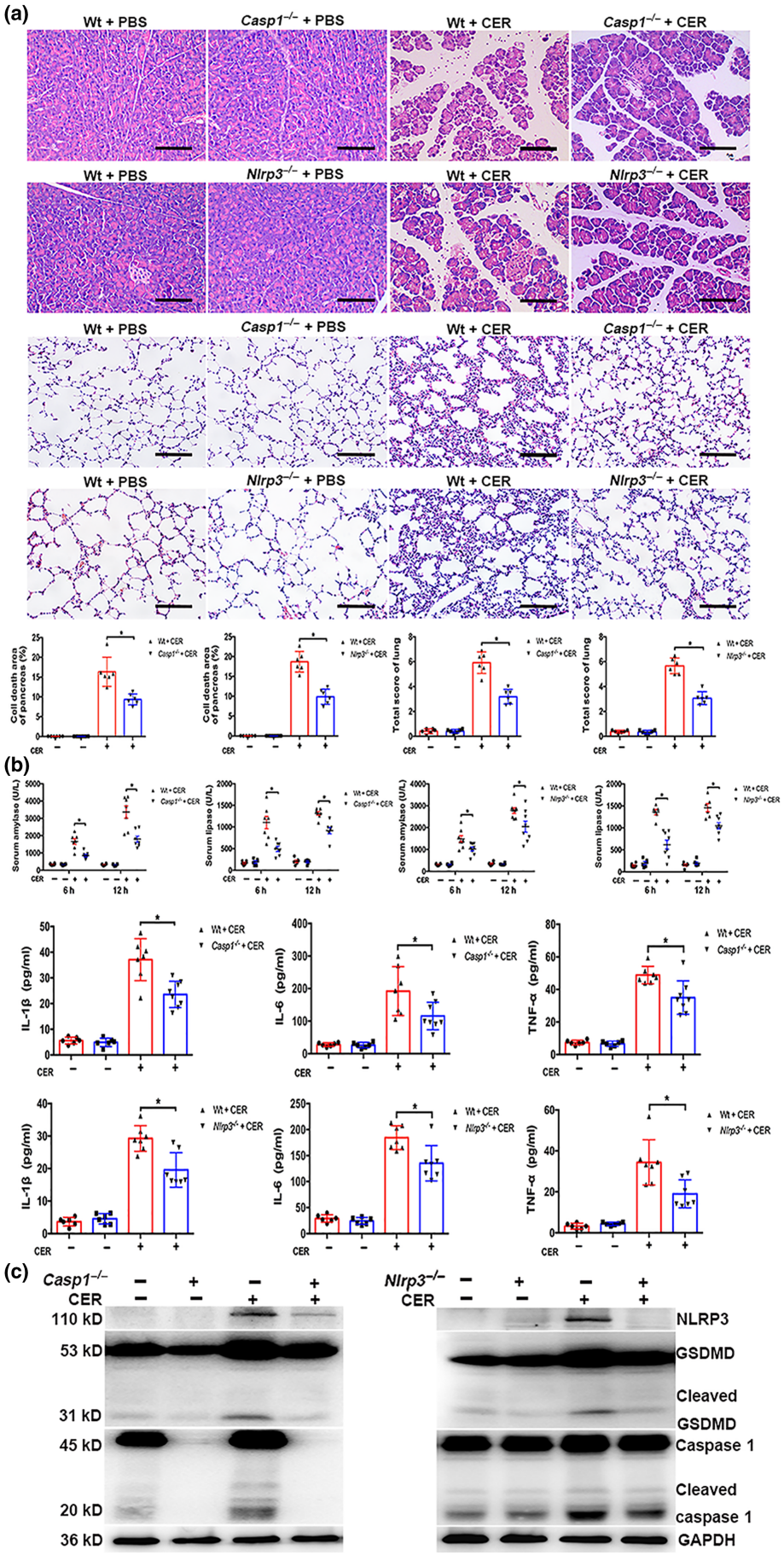

FIGURE 6 Pyroptosis-related gene deletion reduces pancreatic necrosis and systemic inflammation in caerulein-induced AP (CER-AP) in mice. Details for experimental AP induction and severity assessment were described in Section 2. Animals (WT, *Casp1*$^{-/-}$ and *Nlrp3*$^{-/-}$) were killed at 12 h after the first CER/PBS injection. (a) Representative H&E images of pancreas, lung and pancreatic cell death percentages, and total histological scores of lung injury. Scale bar, 100 μm. Data were expressed as mean ± SEM, $n = 6$ per group, $^{*}P < .05$ versus CER. (b) Serum amylase, lipase, and IL-1β, IL-6 and TNF-α levels. Data were expressed as mean ± SEM, $n = 6$ per group, $^{*}P < .05$ versus CER. (c) Western blotting analysis of pyroptosis-related proteins in pancreatic tissues. $n = 6$ per group

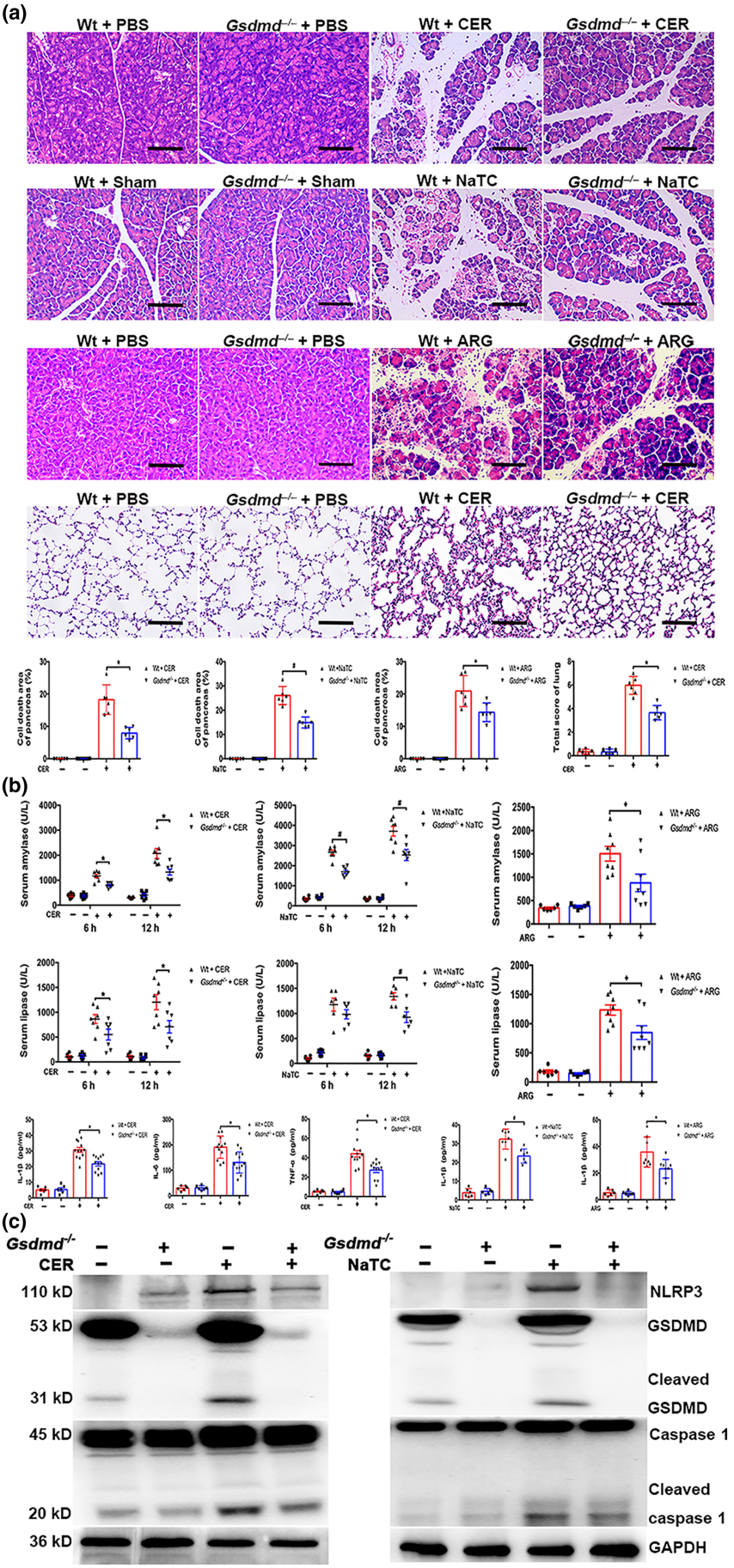

FIGURE 7 *Gsdmd* deficiency reduces pancreatic necrosis and systemic inflammation in three different mouse AP models. Details for experimental AP induction and severity assessment were described in Section 2. Caerulein (CER), sodium taurocholate (NaTC) and L-arginine (ARG) were used to induce AP in mice, and animals (WT and *Gsdmd*$^{-/-}$) were killed at 12, 24 and 72 h for each model, respectively. (a) Representative H&E images of pancreas, pancreatic cell death percentages for each model and representative H&E images of lung, and total histological scores of lung injury for CER-AP. Scale bar, 100 μm. Data were expressed as mean ± SEM, $n = 6$ per group, $^{*}P < .05$ versus CER, $^{\#}P < .05$ versus NATC and $^{+}P < .05$ versus ARG. (b) Serum amylase, lipase and IL-1β levels for each model and serum IL-6 and TNF-α levels for CER-AP. Data were expressed as mean ± SEM, $n = 6$ per group, $^{*}P < .05$ versus CER, $^{\#}P < .05$ versus NATC and $^{+}P < .05$ versus ARG. (c) Western blotting analysis of pyroptosis-related proteins in pancreatic tissues for CER-AP and NaTC-AP. $n = 6$ per group

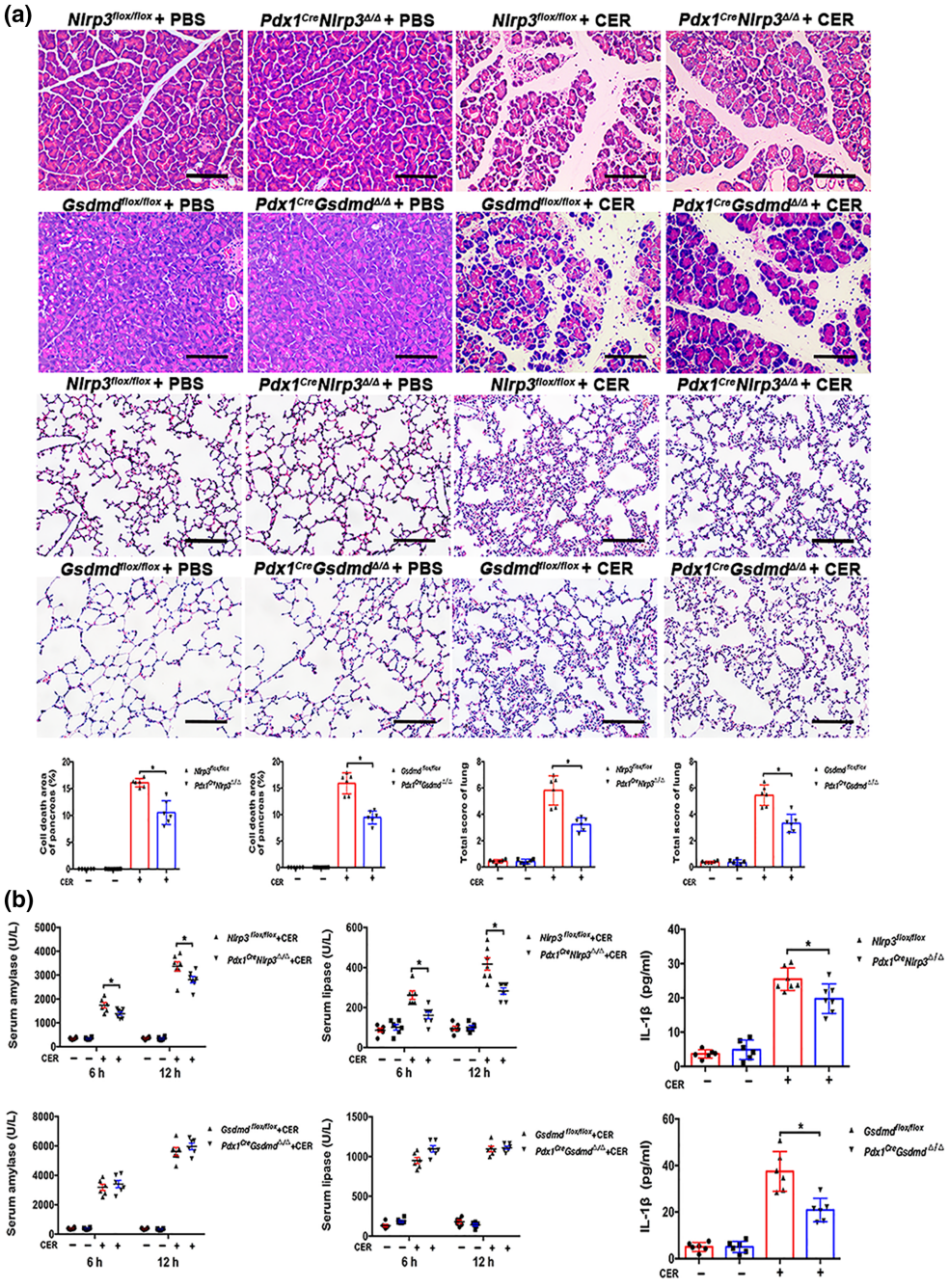

FIGURE 8 Acinar cell-specific *Nlrp3* or *Gsdmd* knockout alleviates pancreatic necrosis and systemic inflammation in caerulein-induced acute pancreatitis (CER-AP) in mice. Details of specific acinar cell *Nlrp3* and *Gsdmd* knockout, caerulein (CER) injections, and severity assessment were described in Section 2. Animals were killed at 12 h after first CER/PBS injection. (a) Representative H&E images of pancreas, lung and pancreatic cell death percentages, and total histological scores of lung injury. Scale bar, 100 μm. Data were expressed as mean ± SEM, $n = 6$ per group, $^*P < .05$ versus CER. (b) Serum amylase, lipase and IL-1β levels. Data were expressed as mean ± SEM, $n = 6$ per group, $^*P < .05$ versus CER. (c) Western blotting analysis of pyroptosis-related proteins in pancreatic tissues. $n = 6$ per group

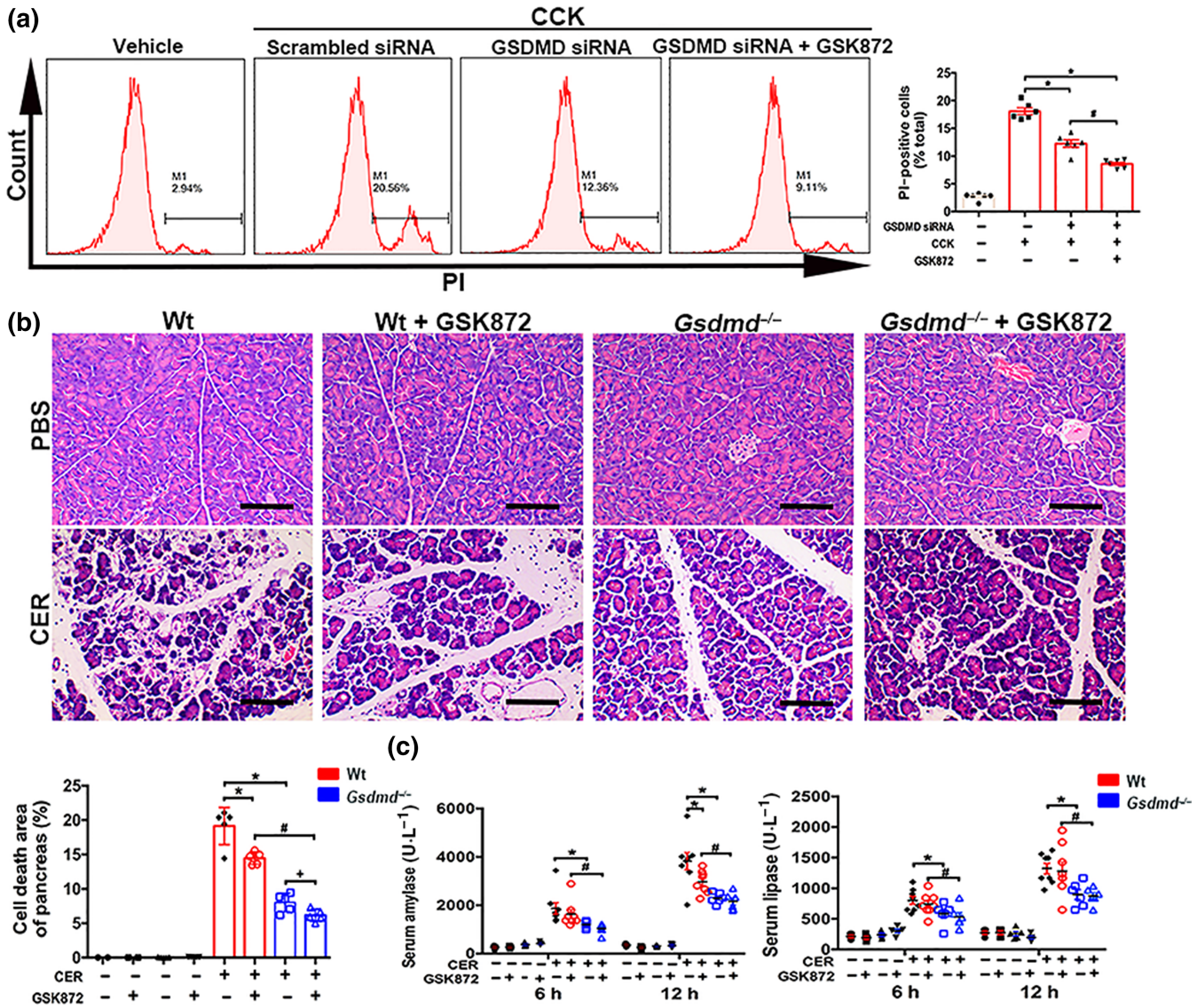

FIGURE 9 Necroptosis inhibition adds more protection to *Gsdmd* knockout mice in caerulein-induced acute pancreatitis (CER-AP) in mice. Details of caerulein (CER) injections and severity assessment were described in Section 2. Animals (WT and $Gsdmd^{-/-}$) were killed at 12 h after first caerulein/PBS injection. (a) Scrambled or gasdermin D (GSDMD) siRNA transfected 266-6 cells were incubated with cholecystokinin (CCK; 8 μM) with or without RIP3 inhibitor GSK842 (2 μM), and necrotic cell death pathway activation was determined by propidium iodide (PI; 4 μM) using flow cytometry. 266-6 cells with only PBS incubation were used as controls (vehicle). Data were expressed as mean ± SEM, $n = 6$ per group, $^{*}P < .05$ versus CCK + scrambled siRNA and $^{\#}P < .05$ versus CCK + GSDMD siRNA. (b) Representative H&E images of pancreas and pancreatic cell death percentages. Scale bar, 100 μm. Data were expressed as mean ± SEM, $n = 5$ per group, $^{*}P < .05$ versus WT + CER, $^{\#}p < .05$ versus WT + CER + GSK872 and $^{+}P < .05$ versus $Gsdmd^{-/-}$ + CER. (c) Serum amylase and lipase levels. Data were expressed as mean ± SEM, $n = 5$ per group, $^{*}P < .05$ versus WT + CER, $^{\#}P < .05$ versus WT + CER + GSK872 and $^{+}P < .05$ versus $Gsdmd^{-/-}$ + CER

([CCK] 18.1 ± 0.6% vs. [GSDMD siRNA] 12.3 ± 0.7%), whereas GSK872 could further significantly reduce PI-positive cells by 20% ([GSDMD siRNA] 12.3 ± 0.7% vs. [GSDMD siRNA + GSK872] 8.6 ± 0.3%) (Figure 9a).

We further validated the above results *in vivo*. In the CER-AP, $Gsdmd^{-/-}$ mice showed much more profound effects in reducing pancreatic necrosis (Figure 9b) and serum pancreatic enzymes (Figure 9c) compared with the necroptosis inhibitor GSK872. The addition of GSK872 to *Gsdmd* genetic deletion reduced pancreatic necrosis further when compared with $Gsdmd^{-/-}$ mice alone, although not for pancreatic enzymes (Figure 9b,c).

Taken together, the roles of pyroptotic acinar cell death and pyroptosis inhibition in are summarised in Figure 10.

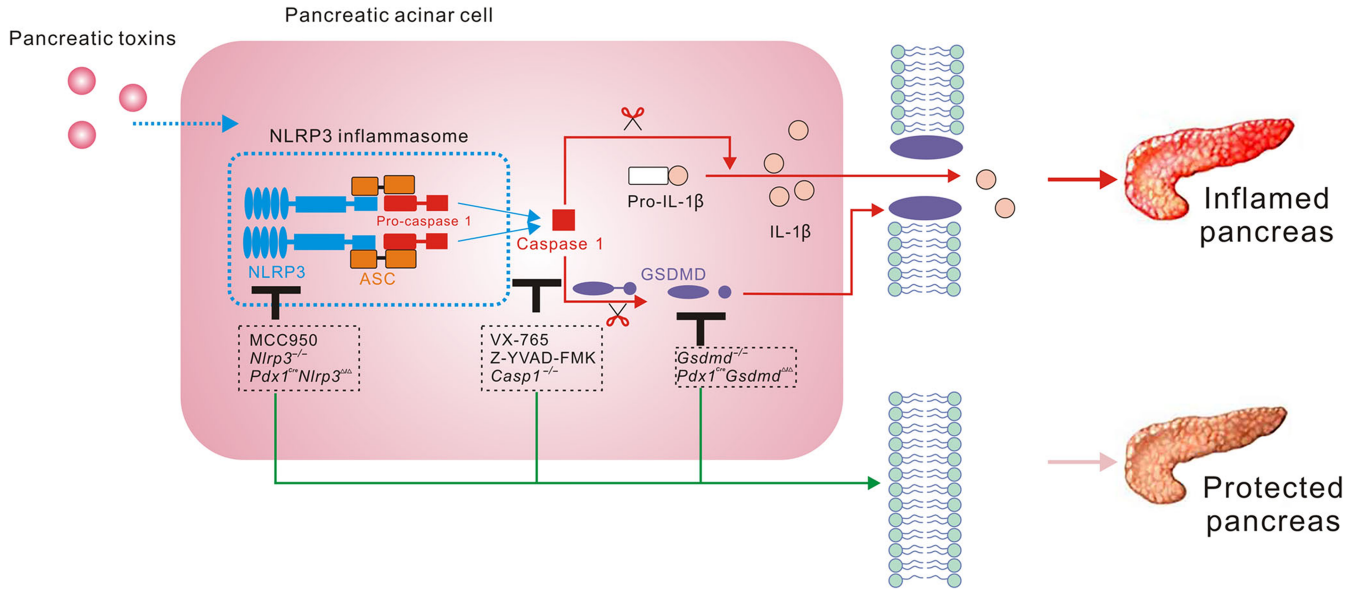

FIGURE 10 The role of acinar pyroptotic cell death and pyroptosis inhibition in acute pancreatitis (AP). In this study, we discovered that there was consistent activation of NLRP3, cleaved caspase 1 and cleaved gasdermin D (GSDMD) when freshly isolated acinar cells and pancreatic acinar carcinoma 266-6 cells were stimulated with cholecystokinin (CCK) or sodium taurocholate (NaTC), implicating induction of pyroptotic cell death activation by common pancreatic toxins. Co-localisation of GSDMD and amylase (a marker for acinar cells) was also detected by immunofluorescent staining in both mouse AP models and human pancreatitis. Genetic deletion of *Gsdmd*, GSDMD knock-down by siRNA and pharmacological inhibition of inflammasome components (NLRP3 or caspase 1) all uniformly suppressed CCK- and NaTC-induced necrotic acinar cell death. In concordance with these *in vitro* findings, we also observed activation of NLRP3, cleaved caspase 1 and cleaved GSDMD in both caerulein- and NaTC-induced AP models at various different time points after disease induction. Further, genetic deletion (*Nlrp3*$^{-/-}$, *Casp1*$^{-/-}$ and *Gsdmd*$^{-/-}$) or pharmacological inhibition (NLRP3-selective inhibitor MCC950 or caspase 1-selective inhibitor VX-765) all significantly reduced pancreatic pyroptotic cell death activation, necrosis and systemic inflammation in various AP models

4 | DISCUSSION AND CONCLUSIONS

This study is the most extensive and detailed of pyroptosis in experimental AP to date, combining *in vitro* and *in vivo* approaches with genetic and pharmacological inhibition of key pyroptotic pathways. We found that significant acinar cell pyroptosis was present in both *in vitro* and *in vivo* models as well as in human pancreatitis tissue, depending on GSDMD activation. Genetic and pharmacological pyroptosis inhibition reduced pyroptotic acinar cell death, pancreatic necrosis and systemic inflammation, which were further reduced by simultaneous inhibition of necroptosis. Interestingly, acinar cell *Nlrp3* or *Gsdmd*, but not myeloid cell *Gsdmd*, conditional knockout significantly protected against pancreatic pyroptotic cell death activation, pancreatic necrosis and systemic inflammation, confirming the importance of acinar cell injury. Taken together, our findings indicate that pancreatic toxin-induced pyroptotic acinar cell death plays a critical role in pancreatic necrosis and systemic inflammation during AP. Therefore, pharmacological therapies targeted at pyroptosis-related proteins including NLRP3 inflammasome components (Mangan et al., 2018) and GSDMD (Qiu et al., 2017) may serve as a promising strategy for AP treatment (Figure 10).

Pancreatic acinar cells are the predominant cell type of the pancreas and the primary victims from injury induced by pancreatic toxins such as CCK (Murphy et al., 2008), bile acids (Voronina et al., 2005) and ethanol metabolites (Huang et al., 2014). Clinically, severe AP represents a classic paradigm of regulated cell death initiating local inflammation, forming a positive auto-amplification loop and ultimately resulting in systemic inflammatory response syndrome and organ failure (Hoque et al., 2011; Linkermann et al., 2014; Liu et al., 2017). Unfortunately, there are no drugs specifically designed to prevent further acinar cell injury, aiming to stop the 'brake' between cell death, inflammation and organ failure. Thus, targeted therapy for AP is urgently needed. In the current study, inhibition of NLRP3 inflammasome components by pharmacological inhibitors exerted both prophylactic and therapeutic effects on AP, demonstrated as reduced pancreatic necrosis and alleviated acute lung injury, which is the most distinguished distant organ failure associated with AP (Shields et al., 2002). These findings justify the translational perspectives of pyroptosis inhibitors in the treatment of AP, especially in the severe mode of AP, which is mainly featured as intensive pancreatic necrosis and organ failure.

Of note, although NLRP3 inflammasome inhibitors have significant effects on acinar cell death and systemic inflammation, they fail to reduce the elevated serum amylase and lipase levels in AP. Amylase and lipase, as markers of pancreatic inflammation, are used to evaluate the severity of AP along with other histological parameters in animal models, but they are not considered clinically as disease severity markers for AP (Leppäniemi et al., 2019).

Several previous animal studies also failed to observe the change in amylase levels despite the significant reduction in distant organ injury and systemic inflammation (de Almeida et al., 2006; de Campos et al., 2008). Besides AP, elevations in amylase and lipase levels could also be caused by critical illness, renal injury (e.g. from reduced excretion) and medications (e.g. calcium channel blockers and corticosteroids) (Alvarez et al., 2019). The effects of NLRP3 inflammasome inhibitors (MCC950 and VX-765) on renal function or promoting the release of amylase and lipase cannot therefore be ruled out.

An early study has shown that components of the inflammasome (ASC, NLRP3 and caspase 1) within pancreatic resident macrophages are activated by ATP released by injured acinar cells via the plasma membrane **purinoceptor P2X7** (Hoque et al., 2011). Another study showed that nucleosome-induced **absent in melanoma 2 (AIM2)**, but not NLRP3, prompts inflammasome activation and subsequent pro-inflammatory mediator release in macrophages (Kang et al., 2016). These studies indicate that inflammasome activation in macrophage plays an important role in the pathogenesis of AP, but the NLRP3 inflammasome activation in pancreatic acinar cells and its role in AP have not been systematically explored before. Inflammasome activation is not restricted to immune cells, as seen in previous studies showing that non-haematopoietic cells, for example, pancreatic acinar cells, rather than haematopoietic cells exhibit NOD1 activity following caspase-1 activation in both murine AP (Tsuji et al., 2012) and chronic pancreatitis (Watanabe et al., 2016). In agreement with these findings, we found the pancreatic acinar cell *Nlrp3* or *Gsdmd*, but not myeloid cell *Gsdmd*, conditional knockout that demonstrated significantly reduced severity of AP. Our study highlights that inflammasome activation and subsequent pyroptosis in pancreatic acinar cells are critical for pancreatic necrosis and systemic inflammation during AP.

It remains unclear whether pyroptosis or necroptosis plays a more important role in pancreatic acinar necrotic cell death. Louhimo et al. declared that under *in vitro* conditions, necrostatin (RIP1 inhibitor) inhibited more than 50% of the cell death upon pancreatic toxin stimulation, which was inconsistent with our findings. In our study, we observed that pyroptosis (caspase 1 and PI double positive) was predominant following CCK or sodium taurocholate exposure. In addition, *Gsdmd* deletion demonstrated more profound effects in reducing pancreatic necrosis when compared with RIP3 inhibitor in CER-AP. There are two potential reasons for this. First, necroptosis inhibitors may have off-target effects, unexpectedly affecting other cell death pathways; second, a crosstalk between necroptosis and pyroptosis in acinar necrotic cell death cannot be ruled out. For example, in human cell lines, MLKL ion channel formation can lead to NLRP3 inflammasome activation in a cell-intrinsic manner, which suggests the presence of crosstalk between pyroptosis and necroptosis (Conos et al., 2017).

In summary, our results showcase the important role of pancreatic acinar GSDMD activation-mediated pyroptosis in linking pancreatic cell death responses and systemic inflammation in AP. Translational drug discovery programmes are awaited to develop novel molecules targeting the NLRP3 inflammasome and GSDMD for clinical AP.

ACKNOWLEDGEMENTS

The authors thank Mr Aihua Zhang from Nanjing Medical University for provision of *Nlrp3*$^{-/-}$ mice and Mr Wenjian Mao for technique assistance. This work was supported by the National Natural Science Foundation of China (81801970, 81570584, 81670588, 81800575 and 81973632) and Jiangsu Provincial Key Research and Development Program (BE2015685 and BE2016749).

AUTHOR CONTRIBUTIONS

L.G. and X.D. performed the experiments; acquired, analysed and interpreted the data; and drafted the manuscript. W.G., W.H. and J.S. acquired, analysed and interpreted the data and drafted the manuscript. N.M., W.C. and Q.Z. acquired, analysed and interpreted the data. J.X., X.F., Y.D., X.G., Z.L. and T.L. provided material or technique support and critically revised the manuscript. Z.T. critically revised the manuscript and obtained funding. R.M. and R.S. critically revised the manuscript. G.L. and W.L. conceived, designed and supervised the study; analysed and interpreted the data; critically revised the manuscript; and obtained funding.

CONFLICT OF INTEREST

The authors declare no competing financial interests in relation to the work described.

DECLARATION OF TRANSPARENCY AND SCIENTIFIC RIGOUR

This Declaration acknowledges that this paper adheres to the principles for transparent reporting and scientific rigour of preclinical research as stated in the *BJP* guidelines for Design & Analysis, Immunoblotting and Immunochemistry and Animal Experimentation and as recommended by funding agencies, publishers and other organisations engaged with supporting research.

DATA AVAILABILITY STATEMENT

The data that support the findings of this study are available from the corresponding author upon reasonable request (Guotao Lu: pkulgt@163.com). Some data may not be made available because of privacy or ethical restrictions.

ORCID

Xianghui Fu https://orcid.org/0000-0001-9808-3892
Weiqin Li https://orcid.org/0000-0002-8483-6264

REFERENCES

Alexander, S. P. H., Kelly, E., Mathie, A., Peters, J. A., Veale, E. L., Armstrong, J. F., Faccenda, E., Harding, S. D., Pawson, A. J., Sharman, J. L., Southan, C., Buneman, O. P., Cidlowski, J. A., Christopoulos, A., Davenport, A. P., Fabbro, D., Spedding, M., Striessnig, J., Davies, J. A., & CGTP Collaborators. (2019). The Concise

Guide to PHARMACOLOGY 2019/20: Introduction and other protein targets. *British Journal of Pharmacology*, *176*(Suppl 1), S1–S20.

Alexander, S. P. H., Roberts, R. E., Broughton, B. R. S., Sobey, C. G., George, C. H., Stanford, S. C., Cirino, G., Docherty, J. R., Giembycz, M. A., Hoyer, D., Insel, P. A., Izzo, A. A., Ji, Y., MacEwan, D., Mangum, J., Wonnacott, S., & Ahluwalia, A. (2018). Goals and practicalities of immunoblotting and immunohistochemistry: A guide for submission to the *British Journal of Pharmacology*. *British Journal of Pharmacology*, *175*, 407–411. https://doi.org/10.1111/bph.14112

Alvarez, E., Persaud, R., Soniega-Sherwood, J., Rattray, J., & Richman, M. (2019). Critical illness causing marked hyperlipasemia. *The American Journal of Medicine*, *132*, e540–e541. https://doi.org/10.1016/j.amjmed.2018.12.006

Banks, P. A., Bollen, T. L., Dervenis, C., Gooszen, H. G., Johnson, C. D., Sarr, M. G., Tsiotos, G. G., Vege, S. S., & Acute Pancreatitis Classification Working Group. (2013). Classification of acute pancreatitis—2012: Revision of the Atlanta classification and definitions by international consensus. *Gut*, *62*, 102–111. https://doi.org/10.1136/gutjnl-2012-302779

Chang, Y. Y., Kao, M. C., Lin, J. A., Chen, T. Y., Cheng, C. F., Wong, C. S., Tzeng, I. S., & Huang, C. J. (2018). Effects of $MgSO_4$ on inhibiting Nod-like receptor protein 3 inflammasome involve decreasing intracellular calcium. *The Journal of Surgical Research*, *221*, 257–265. https://doi.org/10.1016/j.jss.2017.09.005

Coll, R. C., Robertson, A. A., Chae, J. J., Higgins, S. C., Munoz-Planillo, R., Inserra, M. C., Vetter, I., Dungan, L. S., Monks, B. G., Stutz, A., Croker, D. E., Butler, M. S., Haneklaus, M., Sutton, C. E., Núñez, G., Latz, E., Kastner, D. L., Mills, K. H. G., Masters, S. L., … O'Neill, L. A. J. (2015). A small-molecule inhibitor of the NLRP3 inflammasome for the treatment of inflammatory diseases. *Nature Medicine*, *21*, 248–255. https://doi.org/10.1038/nm.3806

Conos, S. A., Chen, K. W., De Nardo, D., Hara, H., Whitehead, L., Nunez, G., Masters, S. L., Murphy, J. M., Schroder, K., Vaux, D. L., Lawlor, K. E., Lindqvist, L. M., & Vince, J. E. (2017). Active MLKL triggers the NLRP3 inflammasome in a cell-intrinsic manner. *Proceedings of the National Academy of Sciences of the United States of America*, *114*, E961–E969. https://doi.org/10.1073/pnas.1613305114

Criddle, D. N., Gerasimenko, J. V., Baumgartner, H. K., Jaffar, M., Voronina, S., Sutton, R., Petersen, O. H., & Gerasimenko, O. V. (2007). Calcium signalling and pancreatic cell death: Apoptosis or necrosis? *Cell Death and Differentiation*, *14*, 1285–1294. https://doi.org/10.1038/sj.cdd.4402150

Curtis, M. J., Alexander, S., Cirino, G., Docherty, J. R., George, C. H., Giembycz, M. A., Hoyer, D., Insel, P. A., Izzo, A. A., Ji, Y., MacEwan, D. J., Sobey, C. G., Stanford, S. C., Teixeira, M. M., Wonnacott, S., & Ahluwalia, A. (2018). Experimental design and analysis and their reporting II: Updated and simplified guidance for authors and peer reviewers. *British Journal of Pharmacology*, *175*, 987–993. https://doi.org/10.1111/bph.14153

de Almeida, J. L., Jukemura, J., Coelho, A. M., Patzina, R. A., Machado, M. C., & da Cunha, J. E. (2006). Inhibition of cyclooxygenase-2 in experimental severe acute pancreatitis. *Clinics (Sao Paulo, Brazil)*, *61*, 301–306.

de Campos, T., Deree, J., Martins, J. O., Loomis, W. H., Shenvi, E., Putnam, J. G., & Coimbra, R. (2008). Pentoxifylline attenuates pulmonary inflammation and neutrophil activation in experimental acute pancreatitis. *Pancreas*, *37*, 42–49. https://doi.org/10.1097/MPA.0b013e3181612d19

Ding, J., Wang, K., Liu, W., She, Y., Sun, Q., Shi, J., Sun, H., Wang, D. C., & Shao, F. (2016). Pore-forming activity and structural autoinhibition of the gasdermin family. *Nature*, *535*, 111–116. https://doi.org/10.1038/nature18590

Gao, L., Lu, G. T., Lu, Y. Y., Xiao, W. M., Mao, W. J., Tong, Z. H., Yang, N., Li, B. Q., Yang, Q., Ding, Y. B., & Li, W. Q. (2018). Diabetes aggravates acute pancreatitis possibly via activation of NLRP3 inflammasome in db/db mice. *American Journal of Translational Research*, *10*, 2015–2025.

Gukovskaya, A. S., Gukovsky, I., Algul, H., & Habtezion, A. (2017). Autophagy, inflammation, and immune dysfunction in the pathogenesis of pancreatitis. *Gastroenterology*, *153*, 1212–1226. https://doi.org/10.1053/j.gastro.2017.08.071

Guo, H., Callaway, J. B., & Ting, J. P. (2015). Inflammasomes: Mechanism of action, role in disease, and therapeutics. *Nature Medicine*, *21*, 677–687. https://doi.org/10.1038/nm.3893

He, W. T., Wan, H., Hu, L., Chen, P., Wang, X., Huang, Z., Yang, Z. H., Zhong, C. Q., & Han, J. (2015). Gasdermin D is an executor of pyroptosis and required for interleukin-1β secretion. *Cell Research*, *25*, 1285–1298. https://doi.org/10.1038/cr.2015.139

Hoque, R., Sohail, M., Malik, A., Sarwar, S., Luo, Y., Shah, A., Barrat, F., Flavell, R., Gorelick, F., Husain, S., & Mehal, W. (2011). TLR9 and the NLRP3 inflammasome link acinar cell death with inflammation in acute pancreatitis. *Gastroenterology*, *141*, 358–369. https://doi.org/10.1053/j.gastro.2011.03.041

Huang, W., Booth, D. M., Cane, M. C., Chvanov, M., Javed, M. A., Elliott, V. L., Armstrong, J. A., Dingsdale, H., Cash, N., Li, Y., Greenhalf, W., Mukherjee, R., Kaphalia, B. S., Jaffar, M., Petersen, O. H., Tepikin, A. V., Sutton, R., & Criddle, D. N. (2014). Fatty acid ethyl ester synthase inhibition ameliorates ethanol-induced Ca^{2+}-dependent mitochondrial dysfunction and acute pancreatitis. *Gut*, *63*, 1313–1324. https://doi.org/10.1136/gutjnl-2012-304058

Huang, W., Cane, M. C., Mukherjee, R., Szatmary, P., Zhang, X., Elliott, V., Ouyang, Y., Chvanov, M., Latawiec, D., Wen, L., Booth, D. M., Haynes, A. C., Petersen, O. H., Tepikin, A. V., Criddle, D. N., & Sutton, R. (2017). Caffeine protects against experimental acute pancreatitis by inhibition of inositol 1,4,5-trisphosphate receptor-mediated Ca^{2+} release. *Gut*, *66*, 301–313. https://doi.org/10.1136/gutjnl-2015-309363

Kaiser, A. M., Saluja, A. K., Sengupta, A., Saluja, M., & Steer, M. L. (1995). Relationship between severity, necrosis, and apoptosis in five models of experimental acute pancreatitis. *The American Journal of Physiology*, *269*, C1295–C1304. https://doi.org/10.1152/ajpcell.1995.269.5.C1295

Kang, R., Chen, R., Xie, M., Cao, L., Lotze, M. T., Tang, D., & Zeh, H. J. III (2016). The receptor for advanced glycation end products activates the AIM2 inflammasome in acute pancreatitis. *Journal of Immunology*, *196*, 4331–4337. https://doi.org/10.4049/jimmunol.1502340

Kayagaki, N., Stowe, I. B., Lee, B. L., O'Rourke, K., Anderson, K., Warming, S., Cuellar, T., Haley, B., Roose-Girma, M., Phung, Q. T., Liu, P. S., Lill, J. R., Li, H., Wu, J., Kummerfeld, S., Zhang, J., Lee, W. P., Snipas, S. J., Salvesen, G. S., … Dixit, V. M. (2015). Caspase-11 cleaves gasdermin D for non-canonical inflammasome signalling. *Nature*, *526*, 666–671. https://doi.org/10.1038/nature15541

Kui, B., Balla, Z., Vasas, B., Vegh, E. T., Pallagi, P., Kormanyos, E. S., Venglovecz, V., Iványi, B., Takács, T., & Péter Hegyi, Z. R. Jr. (2015). New insights into the methodology of L-arginine-induced acute pancreatitis. *PLoS One*, *10*, e0117588. https://doi.org/10.1371/journal.pone.0117588

Lee, P. J., & Papachristou, G. I. (2019). New insights into acute pancreatitis. *Nature Reviews. Gastroenterology & Hepatology*, *16*, 479–496. https://doi.org/10.1038/s41575-019-0158-2

Leppäniemi, A., Tolonen, M., Tarasconi, A., Segovia-Lohse, H., Gamberini, E., Kirkpatrick, A. W., Ball, C. G., Parry, N., Sartelli, M., Wolbrink, D., van Goor, H., Baiocchi, G., Ansaloni, L., Biffl, W., Coccolini, F., di Saverio, S., Kluger, Y., Moore, E., & Catena, F. (2019). 2019 WSES guidelines for the management of severe acute pancreatitis. *World Journal of Emergency Surgery: WJES*, *14*, 27–46. https://doi.org/10.1186/s13017-019-0247-0

Li, J., Zhao, J., Xu, M., Li, M., Wang, B., Qu, X., Yu, C., Hang, H., Xia, Q., Wu, H., Sun, X., Gu, J., & Kong, X. (2020). Blocking GSDMD processing

in innate immune cells but not in hepatocytes protects hepatic ischemia–reperfusion injury. *Cell Death & Disease*, *11*(4), 244–256.

Lilley, E., Stanford, S. C., Kendall, D. E., Alexander, S. P., Cirino, G., Docherty, J. R., George, C. H., Insel, P. A., Izzo, A. A., Ji, Y., Panettieri, R. A., Sobey, C. G., Stefanska, B., Stephens, G., Teixeira, M., & Ahluwalia, A. (2020). ARRIVE 2.0 and the British Journal of Pharmacology: Updated guidance for 2020. *British Journal of Pharmacology*, *177*(16), 3611–3616. https://doi.org/10.1111/bph.15178

Linkermann, A., Stockwell, B. R., Krautwald, S., & Anders, H. J. (2014). Regulated cell death and inflammation: An auto-amplification loop causes organ failure. *Nature Reviews. Immunology*, *14*, 759–767. https://doi.org/10.1038/nri3743

Liu, T., Huang, W., Szatmary, P., Abrams, S. T., Alhamdi, Y., Lin, Z., Greenhalf, W., Wang, G., Sutton, R., & Toh, C. H. (2017). Accuracy of circulating histones in predicting persistent organ failure and mortality in patients with acute pancreatitis. *The British Journal of Surgery*, *104*, 1215–1225. https://doi.org/10.1002/bjs.10538

Liu, X., Zhu, Q., Zhang, M., Yin, T., Xu, R., Xiao, W., Wu, J., Deng, B., Gao, X., Gong, W., Lu, G., & Ding, Y. (2018). Isoliquiritigenin ameliorates acute pancreatitis in mice via inhibition of oxidative stress and modulation of the Nrf2/HO-1 pathway. *Oxidative Medicine and Cellular Longevity*, *2018*, 7161592.

Louhimo, J., Steer, M. L., & Perides, G. (2016). Necroptosis is an important severity determinant and potential therapeutic target in experimental severe pancreatitis. *Cellular and Molecular Gastroenterology and Hepatology*, *2*, 519–535. https://doi.org/10.1016/j.jcmgh.2016.04.002

Ma, C., Yang, D., Wang, B., Wu, C., Wu, Y., Li, S., Liu, X., Lassen, K., Dai, L., & Yang, S. (2020). Gasdermin D in macrophages restrains colitis by controlling cGAS-mediated inflammation. *Science Advances*, *6*, eaaz6717–6730.

Machicado, J. D., Gougol, A., Stello, K., Tang, G., Park, Y., Slivka, A., Whitcomb, D. C., Yadav, D., & Papachristou, G. I. (2017). Acute pancreatitis has a long-term deleterious effect on physical health related quality of life. *Clinical Gastroenterology and Hepatology*, *15*(1435–1443), e1432.

Mandal, P., Berger, S. B., Pillay, S., Moriwaki, K., Huang, C., Guo, H., Lich, J. D., Finger, J., Kasparcova, V., Votta, B., Ouellette, M., King, B. W., Wisnoski, D., Lakdawala, A. S., DeMartino, M. P., Casillas, L. N., Haile, P. A., Sehon, C. A., Marquis, R. W., … Kaiser, W. J. (2014). RIP3 induces apoptosis independent of pronecrotic kinase activity. *Molecular Cell*, *56*, 481–495. https://doi.org/10.1016/j.molcel.2014.10.021

Mangan, M. S. J., Olhava, E. J., Roush, W. R., Seidel, H. M., Glick, G. D., & Latz, E. (2018). Targeting the NLRP3 inflammasome in inflammatory diseases. *Nature Reviews Drug Discovery*, *17*, 588–606. https://doi.org/10.1038/nrd.2018.97

McKenzie, B. A., Mamik, M. K., Saito, L. B., Boghozian, R., Monaco, M. C., Major, E. O., Lu, J.-Q., Branton, W. G., & Power, C. (2018). Caspase-1 inhibition prevents glial inflammasome activation and pyroptosis in models of multiple sclerosis. *Proceedings of the National Academy of Sciences of the United States of America*, *115*, E6065–E6074. https://doi.org/10.1073/pnas.1722041115

Moggia, E., Koti, R., Belgaumkar, A. P., Fazio, F., Pereira, S. P., Davidson, B. R., & Gurusamy, K. S. (2017). Pharmacological interventions for acute pancreatitis. *Cochrane Database of Systematic Reviews*, *4*, CD011384.

Mukherjee, R., Mareninova, O. A., Odinokova, I. V., Huang, W., Murphy, J., Chvanov, M., Javed, M. A., Wen, L., Booth, D. M., Cane, M. C., Awais, M., Gavillet, B., Pruss, R. M., Schaller, S., Molkentin, J. D., Tepikin, A. V., Petersen, O. H., Pandol, S. J., Gukovsky, I., … NIHR Pancreas Biomedical Research Unit. (2016). Mechanism of mitochondrial permeability transition pore induction and damage in the pancreas: Inhibition prevents acute pancreatitis by protecting production of ATP. *Gut*, *65*, 1333–1346. https://doi.org/10.1136/gutjnl-2014-308553

Murphy, J. A., Criddle, D. N., Sherwood, M., Chvanov, M., Mukherjee, R., McLaughlin, E., Booth, D., Gerasimenko, J. V., Raraty, M. G. T., Ghaneh, P., Neoptolemos, J. P., Gerasimenko, O. V., Tepikin, A. V., Green, G. M., Reeve, J. R. Jr., Petersen, O. H., & Sutton, R. (2008). Direct activation of cytosolic Ca^{2+} signaling and enzyme secretion by cholecystokinin in human pancreatic acinar cells. *Gastroenterology*, *135*, 632–641. https://doi.org/10.1053/j.gastro.2008.05.026

Pan, Y., Li, Y., Gao, L., Tong, Z., Ye, B., Liu, S., Li, B., Chen, Y., Yang, Q., Meng, L., Wang, Y., Liu, G., Lu, G., Li, W., & Li, J. (2017). Development of a novel model of hypertriglyceridemic acute pancreatitis in mice. *Scientific Reports*, *7*, 40799. https://doi.org/10.1038/srep40799

Pasparakis, M., & Vandenabeele, P. (2015). Necroptosis and its role in inflammation. *Nature*, *517*, 311–320. https://doi.org/10.1038/nature14191

Percie du Sert, N., Hurst, V., Ahluwalia, A., Alam, S., Avey, M. T., Baker, M., Browne, W. J., Clark, A., Cuthill, I. C., Dirnagl, U., Emerson, M., Garner, P., Holgate, S. T., Howells, D. W., Karp, N. A., Lazic, S. E., Lidster, K., MacCallum, C. J., Macleod, M., … Würbel, H. (2020). The ARRIVE guidelines 2.0: Updated guidelines for reporting animal research. *PLoS Biology*, *18*(7), e3000410. https://doi.org/10.1371/journal.pbio.3000410

Perides, G., van Acker, G. J., Laukkarinen, J. M., & Steer, M. L. (2010). Experimental acute biliary pancreatitis induced by retrograde infusion of bile acids into the mouse pancreatic duct. *Nature Protocols*, *5*, 335–341. https://doi.org/10.1038/nprot.2009.243

Petrov, M. S., & Yadav, D. (2019). Global epidemiology and holistic prevention of pancreatitis. *Nature Reviews Gastroenterology & Hepatology*, *16*, 175–184. https://doi.org/10.1038/s41575-018-0087-5

Qiu, S., Liu, J., & Xing, F. (2017). 'Hints' in the killer protein gasdermin D: Unveiling the secrets of gasdermins driving cell death. *Cell Death and Differentiation*, *24*, 588–596. https://doi.org/10.1038/cdd.2017.24

Schepers, N. J., Bakker, O. J., Besselink, M. G., Ahmed Ali, U., Bollen, T. L., Gooszen, H. G., van Santvoort, H., Bruno, M. J., & Dutch Pancreatitis Study Group. (2019). Impact of characteristics of organ failure and infected necrosis on mortality in necrotising pancreatitis. *Gut*, *68*, 1044–1051. https://doi.org/10.1136/gutjnl-2017-314657

Schroder, K., & Tschopp, J. (2010). The inflammasomes. *Cell*, *140*, 821–832. https://doi.org/10.1016/j.cell.2010.01.040

Shi, J., Zhao, Y., Wang, K., Shi, X., Wang, Y., Huang, H., Zhuang, Y., Cai, T., Wang, F., & Shao, F. (2015). Cleavage of GSDMD by inflammatory caspases determines pyroptotic cell death. *Nature*, *526*, 660–665. https://doi.org/10.1038/nature15514

Shi, N., Liu, T., de la Iglesia-Garcia, D., Deng, L., Jin, T., Lan, L., Zhu, P., Hu, W., Zhou, Z., Singh, V., Dominguez-Munoz, J. E., Windsor, J., Huang, W., Xia, Q., & Sutton, R. (2019). Duration of organ failure impacts mortality in acute pancreatitis. *Gut*, *69*(3), 604–605.

Shields, C. J., Winter, D. C., & Redmond, H. P. (2002). Lung injury in acute pancreatitis: Mechanisms, prevention, and therapy. *Current Opinion in Critical Care*, *8*, 158–163. https://doi.org/10.1097/00075198-200204000-00012

Talukdar, R., Sareen, A., Zhu, H., Yuan, Z., Dixit, A., Cheema, H., George, J., Barlass, U., Sah, R., Garg, S. K., Banerjee, S., Garg, P., Dudeja, V., Dawra, R., & Saluja, A. K. (2016). Release of cathepsin B in cytosol causes cell death in acute pancreatitis. *Gastroenterology*, *151*(747–758), e745.

Tsuji, Y., Watanabe, T., Kudo, M., Arai, H., Strober, W., & Chiba, T. (2012). Sensing of commensal organisms by the intracellular sensor NOD1 mediates experimental pancreatitis. *Immunity*, *37*, 326–338. https://doi.org/10.1016/j.immuni.2012.05.024

van Dijk, S. M., Hallensleben, N. D. L., van Santvoort, H. C., Fockens, P., van Goor, H., Bruno, M. J., Besselink, M. G., & Dutch Pancreatitis Study Group. (2017). Acute pancreatitis: Recent advances through

randomised trials. *Gut*, *66*, 2024–2032. https://doi.org/10.1136/gutjnl-2016-313595

Voronina, S. G., Gryshchenko, O. V., Gerasimenko, O. V., Green, A. K., Petersen, O. H., & Tepikin, A. V. (2005). Bile acids induce a cationic current, depolarizing pancreatic acinar cells and increasing the intracellular Na^+ concentration. *The Journal of Biological Chemistry*, *280*, 1764–1770. https://doi.org/10.1074/jbc.M410230200

Watanabe, T., Sadakane, Y., Yagama, N., Sakurai, T., Ezoe, H., Kudo, M., Chiba, T., & Strober, W. (2016). Nucleotide-binding oligomerization domain 1 acts in concert with the cholecystokinin receptor agonist, cerulein, to induce IL-33-dependent chronic pancreatitis. *Mucosal Immunology*, *9*, 1234–1249. https://doi.org/10.1038/mi.2015.144

Wen, L., Voronina, S., Javed, M. A., Awais, M., Szatmary, P., Latawiec, D., Chvanov, M., Collier, D., Huang, W., Barrett, J., Begg, M., Stauderman, K., Roos, J., Grigoryev, S., Ramos, S., Rogers, E., Whitten, J., Velicelebi, G., Dunn, M., … Sutton, R. (2015). Inhibitors of ORAI1 prevent cytosolic calcium-associated injury of human pancreatic acinar cells and acute pancreatitis in 3 mouse models. *Gastroenterology*, *149*(481–492), e487.

Wu, J., Huang, Z., Ren, J., Zhang, Z., He, P., Li, Y., Ma, J., Chen, W., Zhang, Y., Zhou, X., Yang, Z., Wu, S. Q., Chen, L., & Han, J. (2013). *Mlkl* knockout mice demonstrate the indispensable role of Mlkl in necroptosis. *Cell Research*, *23*, 994–1006. https://doi.org/10.1038/cr.2013.91

Xue, J., Nguyen, D. T., & Habtezion, A. (2012). Aryl hydrocarbon receptor regulates pancreatic IL-22 production and protects mice from acute pancreatitis. *Gastroenterology*, *143*, 1670–1680. https://doi.org/10.1053/j.gastro.2012.08.051

Zhang, R., Deng, L., Jin, T., Zhu, P., Shi, N., Jiang, K., Li, L., Yang, X., Guo, J., Yang, X., Liu, T., Mukherjee, R., Singh, V. K., Windsor, J. A., Sutton, R., Huang, W., & Xia, Q. (2019). Hypertriglyceridaemia-associated acute pancreatitis: Diagnosis and impact on severity. *HPB: The Official Journal of the International Hepato Pancreato Biliary Association*, *21*, 1240–1249. https://doi.org/10.1016/j.hpb.2019.01.015

Zhou, X., Liu, Z., Cheng, X., Zheng, Y., Zeng, F., & He, Y. (2015). Socs1 and Socs3 degrades Traf6 via polyubiquitination in LPS-induced acute necrotizing pancreatitis. *Cell Death & Disease*, *6*, e2012. https://doi.org/10.1038/cddis.2015.342

SUPPORTING INFORMATION

Additional supporting information may be found online in the Supporting Information section at the end of this article.

How to cite this article: Gao L, Dong X, Gong W, et al. Acinar cell NLRP3 inflammasome and gasdermin D (GSDMD) activation mediates pyroptosis and systemic inflammation in acute pancreatitis. *Br J Pharmacol*. 2021;178:3533–3552. https://doi.org/10.1111/bph.15499